THE UNIVERSITY OF OKLAHOMA

GRADUATE COLLEGE

DETERMINATION OF THE OPTICAL CONSTANTS OF SINGLE CRYSTALS USING A NORMAL INCIDENCE REFLECTANCE MICROSPECTROPHOTOMETER

A DISSERTATION

SUBMITTED TO THE GRADUATE FACULTY

in partial fulfillment of the requirements for the

degree of

DOCTOR OF PHILOSOPHY

By

WILLIAM WILSON SHEPHERD

Norman, Oklahoma

1976

DETERMINATION OF THE OPTICAL CONSTANTS OF SINGLE CRYSTALS USING A NORMAL INCIDENCE REFLECTANCE MICROSPECTROPHOTOMETER

APPROVED BY:

DISSERTATION COMMITTEE

To Fallie

"Facts are the enemies of Truth."

M. Cervantes

ACKNOWLEDGEMENTS

I wish to thank my research advisor, Dr. S. C. Neely, for the help he has given during my graduate studies. Special thanks go to Dr. Carl C. Zinsser and Dr. John C. Thompson for valuable assistance and friendship, and to my parents, O. W. and Imogene A. Shepherd, for their devoted support.

Financial assistance from NDEA and from the American Chemical Society - Petroleum Research Fund are gratefully acknowledged. Thanks also go to The Research Corporation for assistance in purchasing necessary equipment.

Most of all, I wish to express my appreciation to my wife, Fallie, whose support was essential for the successful completion of this work. I thank her not only for her assistance in the preparation of the manuscript but also for her understanding and her ability to be patient when appropriate and impatient when appropriate.

TABLE OF CONTENTS

Table of Contents (continued)

LIST OF FIGURES

List of Figures (continued)

List of Figures (continued)

CHAPTER I

INTRODUCTION

In many solid state theoretical problems[25] it is desired to know the value of the optical constants (extinction coefficient and refractive index) of a system as a function of the frequency of the incident radiation. The optical constants quantitatively characterize a transition, and thus may yield information about molecular charge distributions. Since the electrical properties of solids are related to their optical properties,[1] the accurate measurement of the optical constants of strongly absorbing crystals is necessary for the testing of theoretical models of their electronic structure.

Determination of the optical constants of strongly absorbing solids has historically been a difficult problem. In the case of metals, thin prisms of the metal have been used to measure the refractive index,[1] but due to the experimental difficulties such measurements are not very precise and are not generally applicable to organic or inorganic crystals. Direct measurement of absorption is also very difficult, because the incident beam is so heavily attenuated

after passing a short distance through the medium that no signal can be registered by a detector. The situation is improved by making the path length through the sample shorter. Ultimately thin films are necessary in order to achieve a measurable amount of transmitted light. However, thin films do not have the same properties as bulk samples (e.g., crystals), and hence there is frequently no suitable method for measuring absorption directly. In such cases measurable reflectivity can frequently be observed, since strong absorption is usually accompanied by strong reflection.[1] Several methods of determining the refractive index and the extinction coefficient from reflectance measurements have been reported.[2,3,4,5,6,7,8,9,14,15,21,22,23,24]

In the non-normal incidence methods[2,3,6,8] the optical constants may be determined if reflectance measurements are made at two different angles of incidence or if the polarization ratio is measured at one angle of incidence. These techniques have been used in the infrared region of the spectrum but are rarely used in the ultraviolet-visible region. The techniques are tedious, not always accurate in some regions of an absorption band,[2] and cannot be used with small (1 to 2 mm dimensions) crystals as readily as can normal incidence methods.

The normal incidence methods[4,5,7,9,14,15,21,22,23,24] (discussed in chapter IV) all depend on using the Robinson and Price procedure[22] of applying a Kramers-Kronig type

dispersion relation to the data. The method is attractive because of the experimental simplicity, the need for only one reflectance measurement at each frequency, and the fact that smaller crystals may be used. This is the method most commonly used in the UV-visible region for strongly absorbing anisotropic crystals. The major disadvantage of this method is that the calculations depend on a phase angle which is undetermined since data are only available over a finite frequency interval. The differences among the normal incidence methods are due to the manner in which the unobserved spectral "wings" are taken into account. None of the methods provides a generally applicable technique for uniquely determining the adjustable parameters which automatically arise from the wing problem.

Another method of determining optical constants (discussed in chapter IV) using normal incidence reflectance measurements from crystals coated with thin films of known refractive index was introduced by Vincent-Geisse et al.[21,28] Working in the IR spectral region, they used a procedure in which normal incidence reflectance measurements were made successively on first a bare crystal, secondly on the crystal overlaid with a thin film of a transparent solid of known thickness (about 1/4 wavelength) and known refractive index, and finally on the crystal overlaid with two thicknesses of the transparent solid. Their procedure appears to have attracted little attention, probably be-

cause of the experimental difficulty of applying the solid layers to the crystal (which they do by a vapor deposition technique), measuring the thickness of the layers, and the fact that three (more than three in the original version[28]) reflectance measurements are required at each frequency. Schatz, Maeda, et al.[23,24] have also considered the interpretation of reflectance measurements made from a surface covered by a transparent window (refractive index different from air). However, they do not derive the optical constants by comparing reflectances in two different mediums; rather, they modify the usual Kramers-Kronig analysis to allow for the change in reflectance due to the window.

The goal of this research was to develop simple, convenient, generally applicable methods of obtaining reliable optical constants from measurements which could be made with a reflectance microspectrophotometer developed for this project and described in chapter III. This has been achieved by developing a method of reflectance in thick mediums of different refractive index. The required calculations are simple (no integrations are necessary). The experimental procedure is also simple; only two normal incidence reflectance measurements at each frequency are required (one in air and one in a transparent liquid of known refractive index). The experimental procedure for this new method is presented in chapter III; a theoretical discussion and supportive experimental data are presented

in chapter IV. The method becomes extremely error prone in certain regions of the absorption band, so it is suggested this method be used in conjunction with the normal incidence Kramers-Kronig methods to obtain optical constants. Thus, chapter IV contains a review and critical discussion of Kramers-Kronig methods as well as the reflectance in a different medium method.

A molecular crystal of a strongly absorbing chromophore was desired for testing and developing the theory and experimental techniques of the reflectance in a liquid medium method.[1] 1,5-bis-(dimethylamino)pentamethinium perchlorate (called BDP) was chosen; the preparations of it and some other compounds with the same chrompohore are presented in chapter II and appendix C. The chromophore exhibits a strong absorption band (solution extinction coefficient maximum is about 1×10^5 at 4090 Å);[11] the crystal exhibits a broad, metallic reflection band first studied by Anex and Simpson.[13] The electronic states in the molecule and crystal have been further discussed by Neely.[11]

A computer program for the Kramers-Kronig calculation was prepared and optimized for convenience, flexibility, and accuracy; it is included in the appendix as a valuable tool for other workers.

CHAPTER II

PREPARATION OF COMPOUNDS

Because of the previous interest and spectral characterization done[11,12,13,19,26,27] on the 1,5-bis-(dimethylamino)pentamethinium cation chromophore (called BDP^+), its salts were selected for experimental work.

The perchlorate salt of BDP^+ (called BDP) is a starting material for the preparation of other BDP^+ salts. Several attempts were made to synthesize BDP using the method of Feniak[10] as modified by Neely[11] and also by the method described by Malhotra and Whiting.[12] The intermediate aldehyde compound was never successfully recovered in either of these synthesis routes. BDP was finally prepared by a procedure we developed in which 2,4 dinitrophenyl-pyridinium chloride[11] reacts with dimethylamine to yield BDP^+, which is then precipitated by addition of perchlorate. The reaction probably occurs in two steps, the first of which produces an intermediate according to the following equation:

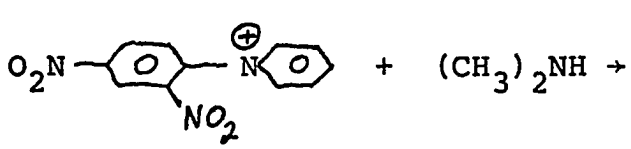

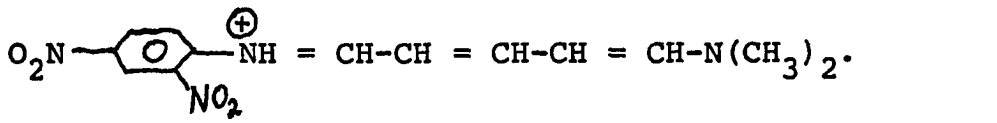

This intermediate then reacts with an additional molecule of $(CH_3)_2NH$ to produce

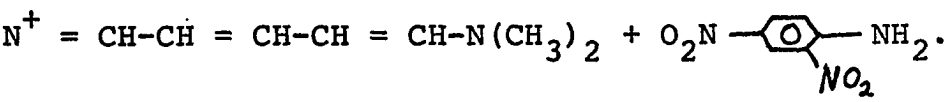

Details of the procedure are as follows: 2,4-dinitrophenylpyridinium chloride (13 g) in ethanol (79 ml) was treated with 40% aqueous dimethylamine (56.5 ml). The mixture was heated at 60°C for 30 minutes with occasional stirring. The mixture was then chilled in ice and 130 ml of water was added. The solid (2,4-dinitroaniline) was filtered and washed with water (two 30 ml portions). The washings were added to the filtrate which was then chilled in ice and acidified with 70% perchloric acid (19 ml). The solid (BDP) was filtered and washed with ether. The yield was 87% based on the 2,4-dinitriphenylpyridinium chloride. Three recrystallizations from methanol gave a bright yellow solid which melted from 163.0 to 165.5°C (literature value 164.0 to 165.5°C). A mixed melting point with this material and some BDP supplied by George Feniak melted at 163 to 165.5°C.

An attempt was made to prepare BDP^+Cl^- using the same method but substituting HCl for the $HClO_4$. However, since this compound is extremely soluble in water, it could not be recovered from the reaction mixture. The Cl^- salt

was made by passing $BDP^+ClO_4^-$ over an ion exchange column of Dowex 2-X8 using a procedure worked out in this lab by S. R. Holbrook. Since $BDP^+ClO_4^-$ is not appreciably soluble in water, the ion exchange column was first treated with a water solution of NaCl, then rinsed with alcohol. The $BDP^+ClO_4^-$ dissolved in alcohol was then passed through the column followed by alcohol rinses. The collected solutions were concentrated in a rotary evaporator, and the compound was precipitated by the addition of diethyl ether. The compound was recrystallized several times by dissolving it in 95% ethanol and then adding diethyl ether. The BDP^+Cl^- melted at 97 to 99°C; its crystal density is 1.126 grams per milliliter.

BDP crystals were grown as described by Neely.[11] Crystals of BDP^+Cl^- were grown by placing the compound in a vial and adding ethanol in excess of the amount required to dissolve the material. Then a small amount of ether was added to bring the solution back to a state of near saturation. This procedure allows the crystals to grow from a more dilute solution than would be possible if only a saturated solution of compound in alcohol were used rather than a mixed solvent. The vial was then covered with perforated aluminum foil. The extent of perforation controls the rate of crystal growth. The covered vial was placed in a jar containing diethyl ether. The jar was capped and allowed to stand a few days.

The method of recovering the crystals from these cells proved to influence the stability of the crystals when exposed to the lab air. If the crystals are simply removed from the cell and discharged onto a pad of filter paper, their reflectivity visibly diminishes in less than a minute. The following technique greatly improves their stability. A small jar is partially filled with anhydrous calcium chloride, and a small filter paper pad is placed on top of the calcium chloride. A hole is cut in the cap large enough to admit a medicine dropper. After the jar sets long enough to produce a dry atmosphere, the crystals and some of the mother liquor are sucked into the medicine dropper and discharged into the drying jar. After the crystals have dried (approximately 15 minutes), they can be removed from the drying jar and exposed to lab air for a few hours with only a slight deterioration. If placed in stoppered vials and stored in a dark area (at room temperature), they can be stored for months with only slight deterioration.

Compounds other than BDP which contain the BDP^+ chromophore would be interesting to study as an extension of work done on BDP, especially if the crystal structure results in a relative configuration of the BDP^+ cations which is different from the configuration in BDP.[11] Methods developed in this lab for preparing the Br^-, I^-, and sulfate salts of BDP^+ are presented in appendix C in anticipation of such investigation.

CHAPTER III

THE REFLECTANCE MICROSPECTROPHOTOMETER

A. Introduction

This instrument was designed to measure the normal incidence plane polarized UV-visible reflection spectrum from faces of single crystals. The general design principles are the same as for the instrument introduced by Anex and Simpson[13] and modified as described by Neely[11] and Fratini.[19] The crystal is appropriately oriented on the stage of a vertically illuminating microscope, and variable frequency monochromatic plane polarized light is used for illumination. The intensity of the reflected light is monitored by a photomultiplier mounted at the top of the microscope barrel. Since this is a single beam system, the observed intensity from the crystal must be compared to the observed intensity (under identical instrumental conditions) from a reference standard of known absolute reflectance.

B. Construction

The instrument is illustrated in figure 3-1. The light sources used are Bausch and Lomb tungsten (quartz-

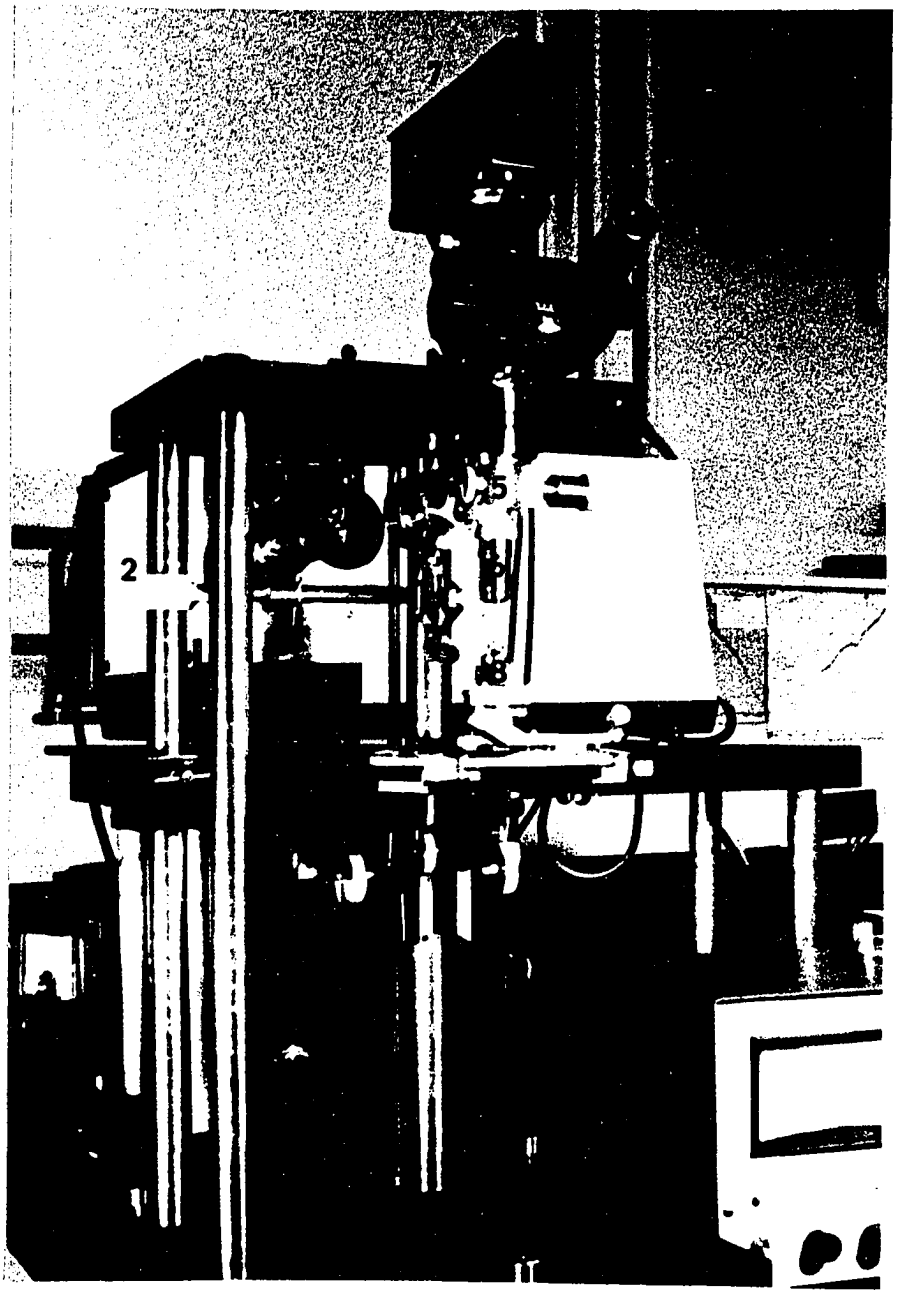

Figure 3-1. Reflectance Microspectrophotometer

1. Light Source
2. Monochromator
3. Condensing Lens
4. Polarizing Prism
5. Verticle Illuminator
6. Microscope Objective
7. Detector
8. Goniometer
9. Iris diaphragm

iodine) source (model 33-86-39-01) for the spectral region from 700 nm to 375 nm and deuterium source (model 33-86-35-01) from 375 nm to 200 nm. Bausch and Lomb markets other sources in the same housing which would be interchangeable with the tungsten and deuterium sources. Different sources may have advantages such as higher intensity in a particular spectral region. The sources mount directly onto the monochromator via a special mounting plate. This facilitates rapid changing of sources without creating alignment problems.

The monochromator is a Heath (model Eu-700-51) scanning monochromator. It is mounted on a stand separate from the microscope stand (both stands are equipped with leveling screws). An achromatic condensing lens (Bausch and Lomb model 33-86-53) is mounted over the exit slit of the monochromator via a special bracket. Use of a condensing lens greatly increases the light intensity of the system. A Glan-Thompson polarizing prism is mounted between the monochromator and the microscope in order to plane polarize the incoming light.

The microscope barrel assembly equipped with vertical illuminator and the circular stage and the rack and pinion assembly are from a Zeiss Ortholux polarizing microscope. The corrective lens was removed from the microscope barrel and the collective lens removed from the vertical illuminator in order to improve UV transmission.

A quartz plate (18 x 12 x 1 mm) was installed in the vertical illuminator as a beam splitter. Commercially available UV transmitting microscope objectives are used. The conventional microscope stand has been replaced by a custom made stand designed and built by Mr. Carl Starkey. The stand features an open area between the vertical illuminator and the monochromator which facilitates mounting the polarizing prism and any other desired attachments such as aperture stops, etc. The main feature of the stand is the fact that the stage rack and pinion assembly is carried on a mounting bracket which rides up and down two shafts. Using this mechanism, the distance from the microscope objective to the top of the mounting bracket can be varied up to 15 inches. This gives a great deal of flexibility as far as mounting various accessories on the stage.

The detector is an Eldorado Electronics differential photometer (model 211). It includes a 1P28 photomultiplier tube in a housing threaded to fit a camera adapter. A special bracket was made to screw into the housing and slide into the camera access at the top of the microscope barrel. The photomultiplier output is monitored by a meter on the amplifier or by a Beckman 10 inch recorder (model 1005) connected to the amplifier.

In order to measure the spectrum in air, a crystal is placed on a plate supported on a goniometer head which is mounted on a translating mechanical stage. This assembly

is attached to the circular stage of the microscope. The motions of the goniometer head provide a convenient means of leveling a crystal face; the crystal face must be oriented normal to the incident light. The translating mechanical stage is used to position the crystal in the light beam and to select a particular area of the face for examination. The circular stage is used to rotate the crystal to the desired orientation with respect to the plane of polarization of the incident light. Since the circular stage is calibrated to show the angle through which it has rotated, it can also be used to determine the crystal polarization angle with respect to a crystal edge.

C. Alignment Procedure

1. Introduction

Good alignment is important for maximum efficiency and performance. Alignment can be frustrating, tedious, time consuming, and even unsuccessful if a proper approach is not used. After much experience, the systematic procedure described below was found to be the most successful and the easiest to perform. The approaches and techniques developed here should be generally useful to the alignment of many spectrophotometer systems.

2. Major Components

A bracket was made which allows the sources to be

attached directly to the Heath monochromator in the same manner as they are designed to mount on the Bausch and Lomb monochromator. Alignment pins are included, so the sources can be removed and replaced reproducibly. Thus, the sources are aligned initially according to the directions supplied by the manufacturer, and no further adjustment is necessary. Next, the monochromator and the microscope stand are leveled and crudely aligned using the edge of the lab bench as a reference line. The height of the monochromator slits above the table top is made equal to the height of the entrance of the vertical illuminator. The condenser lens is removed from the monochromator exit, and white light from the source is passed through the system. The standard mirror is placed on the microscope stage and leveled, and the microscope objective is centered. The entrance to the vertical illuminator is brought to the center of the light beam which is exiting from the monochromator (visual estimation). Alignment can then be considered to be the problem of setting the microscope normal to this beam. Having both the monochromator and the microscope stand level insures that the vertical axis of the microscope is normal to the center line of the monochromator exit beam. The only other adjustment is to rotate the microscope around its vertical axis. However, the system is quite insensitive to a misalignment of this type, and simply squaring the microscope stand with respect to the

edge of the lab bench is sufficiently accurate. Finally, the monochromator slits are brought into focus and centered on the crosshairs by slight movement of the microscope.

3. Condenser Lens

The condenser lens is now mounted over the exit slit of the monochromator, and its focusing tube is extended to its normal position (i.e., the monochromator slits are focused on the entrance to the vertical illuminator). The lens position is adjusted without moving either the monochromator or the microscope. Adjustment is accomplished by shimming or translating the lens mounting bracket. Alignment of the lens is complete when the image of the monochromator slits is again centered on the cross hairs. The iris diaphragm which is mounted over the lens should be closed down, and then observed through the microscope to verify that it is also centered with respect to the cross hairs. It is important to center the condenser lens by this procedure; if this procedure is not followed, it is extremely difficult to center both the monochromator slits and the iris diaphragm onto the cross hairs.

4. Vertical Illuminator

When mounting the quartz beam splitter in the vertical illuminator, it is necessary to remove the beam splitter support assembly from the microscope. When it is

reinstalled it should be realigned by the following procedure. The photomultiplier tube assembly is removed from the microscope, and a thin piece of paper is placed under the aperture stop in order to make the position of the light beam visible. The four mounting screws which secure the beam splitter support assembly are loosened slightly. The assembly is then rotated and/or translated until an image of the iris diaphragm is centered simultaneously on the cross hairs and on the aperture stop. The mounting screws are then carefully tightened. Now, any image which is centered on the cross hairs will also be imaged in the center of the photomultiplier tube aperture stop. If this alignment is not done it is necessary to readjust the angle of the beam splitter while observing the intensity reading on the detector scale each time a crystal is visually aligned. When a small aperture stop is used, the observed intensity is very sensitive to the angle setting, which makes its adjustment tedious. Also, it is easy to forget to make the adjustment. Thus, it is quite advantageous to make this alignment.

5. Polarizing Prism

When the polarizing prism is mounted in the light path, the light beam is displaced a small distance to the side. A small displacement of the microscope stand in the same direction is necessary to restore alignment of the

rest of the system. Since it is desirable to be able to measure the angle of polarization for the crystal, it is necessary to have a visual reference for the plane of polarization of the incident light. There is a large induced polarization in the instrument without the polarizing prism in place. That this induced polarization is caused by the incident light beam reflecting from the quartz plate beam splitter can be seen from the following consideration. The plane of incidence is defined as containing the incident and reflected beams. At an angle of 45 degrees the component of light which has its electric vector perpendicular to the plane of incidence has a reflection coefficient of approximately 9%, while the component with its electric vector in the plane of incidence has a reflection coefficient of approximately 2%.[1] Thus, when unpolarized light strikes the quartz plate at a 45 degree angle the ratio of light polarized perpendicular to the plane of incidence compared to light polarized in the plane of incidence is approximately 4.5 to 1. Note that in this discussion the plane of polarization is defined to contain the electric vector. It is assumed that reflection from the quartz plate is the principle source of induced polarization in the instrument; the degree and direction of polarization induced by other components of the instrument were not investigated. Thus, for maximum efficiency the polarizing prism must be oriented so that its plane of polarization

coincides with the plane of induced polarization. A convenient visual reference line is obtained by closing the monochromator exit slit to a narrow width (200 microns or less), and then bringing the exit slit into visual focus. The cross hairs in the eyepiece are then rotated to make one of the hairs parallel to the image of the slits. The polarizing prism is rotated to approximately the desired position. A clear sheet of plastic is then placed over the polarizer, and a line is marked on the sheet parallel to the edge of the prism. The prism is then rotated until the line on the plastic sheet is parallel to the second cross hair (i.e., perpendicular to the line defined by the monochromator slits). The polarizer is then locked in place with set screws. The angle of polarization with respect to the edge of a crystal is then measured by reading the change in angular setting of the circular stage when the stage is rotated from the position giving maximum reflection to the position which makes the edge of the crystal perpendicular to the exit slit image. The cross hairs are easily misaligned which is the reason for choosing the monochromator slits as the reference for alignment.

D. Optical Characteristics

1. Spectral Response

Instrument response decreases rapidly when going

to wavelengths shorter than 2300 angstroms. This is due primarily to a decrease in photomultiplier tube response at shorter wavelengths and also loss of intensity due to absorption by the polarizing prism at shorter wavelengths. The usable range of the instrument could be extended to shorter wavelengths by using a photomultiplier tube which has better response at short wavelengths and by using a light source which has greater intensity at short wavelengths.

Instrument response decreases rapidly when going to wavelengths longer than 6000 angstroms. This is due primarily to a decrease in photomultiplier tube response at longer wavelengths. The usable range of the instrument could be extended to longer wavelengths by selecting a red sensitive photomultiplier tube and by selecting a monochromator grating blazed at a longer wavelength.

2. Field Stops

The use of field stops insures that any deterioration of optical quality due to the removal of lenses is insignificant, since only a small spot in the center of the field is used during spectrum measurement, whereas the deterioration in image quality occurs mainly towards the edge of the field. There are two mechanisms which insure that only the center of the field is used regardless of how large a crystal is being examined. The condenser lens mounted at

the exit of the monochromator is equipped with an iris diaphragm. By placing the monochromator at a distance from the microscope such that the final distance from the iris diaphragm to the vertical illuminator is equal to the distance from the vertical illuminator to the top of the microscope barrel, an image of the iris diaphragm is focused on the crystal face. This iris diaphragm can then be used to stop down the field being illuminated to only a small spot in the center. The reason that the placement of the iris diaphragm must be as specified above is that when the crystal is in focus, there is an image of the crystal formed at the top of the microscope barrel. Thus, anything placed in the incoming light path at the same optical distance from the crystal as this image will be focused onto the crystal. The second mechanism which insures that only the center of the field is used makes use of the fact that when the crystal is in focus, an image of the crystal is formed at the top of the microscope barrel. This focal point is easily accessible with an aperture stop which is placed immediately in front of the photomultiplier tube. An image was observed by holding a thin piece of paper at this point, and the typical image size was measured. Three millimeters diameter was selected for the size of the stop. An additional benefit of this stop is that since its aperture is much less than the aperture of the photomultiplier tube window, the amount of stray light reaching the

detector is greatly reduced. However, there is practically no reduction in the light which is reflected from the crystal. When using this stop and a reflecting objective, the stray light is usually insignificant for reflectance values greater than ten percent.

3. Vertical Illuminator

In the vertical illuminator, part of the incoming light from the monochromator is reflected by the beam splitter down through the microscope objective onto the crystal (the transmitted portion of the light is lost). The light reflected by the crystal passes back through the objective, and part of it is transmitted by the beam splitter up the microscope barrel to the detector (the reflected portion of this light is lost). Thus, the optical efficiency of the beam splitter has a pronounced effect on the overall light efficiency of the system. The uncoated quartz plate used as a beam splitter in this instrument transmits approximately 84% of the incident light and reflects about 15% (1% is absorbed). Since the light must reflect once from the beam splitter and traverse it once, the overall efficiency is 0.15 x 0.84 = 0.126 or about 13%. Beam splitters are available which both transmit and reflect 45% of the incident light (10% is absorbed). However, their overall efficiency would be 0.45 x 0.45 = 0.20 or about

20%. Thus, use of one of these beam splitters would increase the relative light efficiency of the system by about 54%.

A peculiar optical characteristic of the instrument is that although only one image of the crystal is observed, two images (displaced parallel to the slit image) are observed for the iris diaphragm field stop, the monochromator exit slits, and so on for objects along the incoming light path when they are brought into focus. This phenomenon is annoying during alignment of the instrument, and it is objectionable because it limits the size to which the field of illumination may be reduced (if the iris were closed small enough, two spots would be illuminated). Until the cause was discovered, it also appeared that this could be a significant source of stray light, and hence be detrimental to instrument performance. The problem was found to be in the optical properties of the quartz plate beam splitter. When the incident beam of light strikes the quartz plate, a small part of it is reflected, and a large part is transmitted into the plate. When this transmitted beam strikes the back surface of the plate, part of it is reflected internally. This internally reflected beam then strikes the front surface of the plate where a large part of it is transmitted. This transmitted beam emerges parallel to the initially reflected ray as a result of the front and back surfaces of the plate being parallel

to each other. The displacement between these two beams is a function of the thickness of the quartz plate. That these two beams are indeed of comparable intensity may be shown by calculating the relative intensities from Fresnel's equations for reflection and refraction.[1] In terms of intensities the equations for light polarized with the electric vector perpendicular to the plane of reflection are:

$$I_1 = I_o \frac{\sin^2(\theta_1-\theta_2)}{\sin^2(\theta_1+\theta_2)} \qquad \text{eq. 3-1}$$

and

$$I_2 = I_o \frac{4 \sin^2\theta_2 \cos^2\theta_1}{\sin^2(\theta_1+\theta_2)} , \qquad \text{eq. 3-2}$$

where I_o is the intensity of the incident beam, I_1 is the intensity of the reflected beam, I_2 is the intensity of the refracted beam, θ_1 is the angle of incidence, and θ_2 is the angle of refraction. For the incident beam θ_1 = 45 degrees. θ_2 can be calculated from Snell's law assuming a value of 1.5 for the index of refraction of quartz. Then, sin 45° = 1.5 $\sin\theta_2$; thus θ_2 = 28°. Substituting in eq. 3-1,

$$I_1 = I_o \frac{\sin^2 17°}{\sin^2 73°} = 0.093\ I_o, \text{ or } I_1 = 9.3\%\ I_o.$$

Substituting in eq. 3-2,

$$I_2 = I_o \frac{4 \sin^2 28° \cos^2 45°}{\sin^2 73°} = 0.48\ I_o, \text{ or } I_2 = 48\%\ I_o.$$

When this beam reflects from the second interface, eq. 3-1 is again used with $\theta_1 = 28$ degrees and $\theta_2 = 45$ degrees. Calling the intensity of this internally reflected beam I_3,

$$I_3 = 9.3\%\ I_2 = 0.093 \times 48\%\ I_o = 4.5\%\ I_o$$

Finally, when this beam again encounters the front surface of the quartz plate, the intensity of the refracted beam (defined as I_4) may be calculated from eq. 3-2 with $\theta_1 = 28$ degrees and $\theta_2 = 45$ degrees.

$$I_4 = I_3 \frac{4 \sin^2 45° \cos^2 28°}{\sin^2 73°} = 1.7\ I_3 = 1.7 \times 4.5\%\ I_o = 7.7\%\ I_o.$$

Therefore, the internally reflected beam has an intensity 7.7% of the originally incident light, and the initially reflected beam has an intensity 9.3% of the incident light. Thus, the intensity of the internally reflected beam is 83% of the intensity of the initially reflected beam. The problem can be reduced in magnitude by using a thinner quartz plate, so that the images are closer together. However, there are mechanical difficulties in mounting very thin plates. Preferably a pair of closely spaced prisms

should be used as the beam splitter.

4. Microscope Objectives

Commercially available objectives which are designed for UV light transmission are used. In general, reflecting objectives are preferred, because they are perfectly achromatic and have greater transmission. Objectives are modified by removing their cover plate if one is present; this improves transmission in the UV region. High power objectives are desirable for two reasons. One reason is that a higher power objective has a smaller true field of observation. Thus, smaller crystals can be used. Also, less perfect crystals can be used as long as small areas of high perfection can be found. A second reason high power objectives are desirable is because the depth of field in focus is very short. Thus, reflection from the back surface of the crystal or reflections from internal crystal imperfections are not as likely to interfere. These reflections will be out of focus, and hence they will be reduced by the phototube aperture stop. A disadvantage of high power objectives is that in general they produce a greater angle of incidence.

In the Kramers-Kronig calculations the light beam is assumed to strike the crystal at normal incidence. However, the light beam actually strikes the crystal as a convergent cone of light due to the focusing property of the

microscope objective. The true angle of incidence depends on which objective is being used. If the full aperture of an objective is used, the maximum angle of incidence could be calculated from the known numerical aperture of the objective. However, the microscope optics have been modified, and it is possible that the full aperture is not being used. Also, for reflecting objectives, the Cassegranian mirror blocks out the central part of the beam producing a dark cone within the light cone. Therefore, the maximum angle of incidence was measured experimentally for both the 50x reflecting objective and the 40x fluorite objective, and the minimum angle of incidence was measured for the reflecting objective. This was done by the following procedure. The objective was mounted on the microscope, and white light was passed through the system. A white card was placed on the microscope stage and lowered a few inches from the focal position. The diameter of the resulting light spot was measured. The card was then lowered a measured distance of a few more inches and the diameter of the light spot (now larger) was measured again. The angle from the center of the light cone to the edge of the cone was then calculated from the equation

$$\tan \theta = \frac{\text{half the change in diameter}}{\text{change in distance lowered}}.$$

For the fluorite objective θ was found to be 24 degrees.

For the reflecting objective θ was found to be 28 degrees. For the reflecting objective a dark spot lies in the center of the light spot. The angle to the edge of the dark spot determines the minimum angle of incidence for this objective. This angle was found to be 18 degrees. Thus, for the reflecting objective the angle of incidence ranges from 18 to 28 degrees; for the fluorite objective the angle varies from 0 to 24 degrees. The approximation of normal incidence when using the 50X reflecting objective will be poor in some cases because the sensitivity of the reflection spectrum to a change in angle of incidence depends on the compound and its crystal structure. For the fluorite objective the angle of incidence can be made fairly small simply by placing an aperture stop in the back of the objective. Low power reflecting objectives are available which produce an angle of incidence of about 15 degrees; in some cases this angle may still be undesirably large. Note that the average angle of incidence will not equal the mean of the maximum plus minimum angle. The amount of light at a given angle in a cone of light is proportional to the square of the radius of the circle of light corresponding to that angle. Thus, the average angle of incidence will lie nearer the maximum angle (assuming uniform intensity through the beam).

E. Liquid Medium Technique

It is desirable to be able to measure the reflectance of a crystal immersed in a liquid as well as in air (see section IV. B. 3). The techniques used for measurement in air can be extended to measurement in a liquid by using an oil immersion microscope objective, such as the fluorite objective described above. Although simple in principle, there are some details which require attention. Obviously, a liquid must be selected in which the crystal is insoluble. The liquid must be transparent and have as large an index of refraction as possible (preferably greater than 1.4). The crystal must be firmly mounted so that once it is correctly oriented, it will not be displaced when the liquid is added. If the crystal is mounted on a small wire with glue, then it will not be possible to keep the immersion liquid on top of the crystal. This problem was solved by gluing the crystal on a wire, and then mounting the wire with crystal in a small cup. The glue must be unaffected by the liquid medium. The cup is then filled with the liquid to a level above the tip of the microscope objective and mounted on the goniometer head. An additional benefit of this system is that fairly volatile liquids may be used; it is only necessary that the liquid level in the cup not fall below the tip of the microscope objective while taking measurements. This greatly increases the

number of possible liquids which could be used.

The most serious problem which arises when making reflectance measurements in a liquid medium is a change in the light transmission properties of the system. The source of this problem is the reflection losses which occur at the air-glass interface of the objective lens nearest the crystal. When the air medium is replaced with liquid medium (refractive index greater than 1), the reflection losses are reduced. This increases transmission through the system with the result that measurements made in a liquid medium appear more intense than corresponding measurements made in air. This error can be eliminated by comparing crystal readings to reference mirror readings both made in the liquid if the absolute reflectance of the reference mirror in the liquid is known. It cannot be assumed that the reflectivity of the reference mirror will be the same in a liquid as it is in air. If the refractive index of the liquid and of the lens in the objective are known, then the reflection losses at the lens-medium interface can be calculated from Fresnel's equation (4-28),

$$R_{\text{interface}} = \left[\frac{n_1 - n_2}{n_1 + n_2}\right]^2 .$$

A typical refractive index for the front lens of an immersion objective is 1.5,[18] and this is the value assumed for the fluorite objective used for the data re-

ported herein. When iso-octane (refractive index 1.39) is used as the liquid medium,

$$R_{interface} = \left[\frac{1.5-1.39}{1.5+1.39}\right]^2 = .00145.$$

Transmittance, $T = 1-R = .99855$.

This loss occurs each time the light beam crosses the interface. Since the light beam crosses the interface twice (once on the way to the crystal and once on its way to the detector) the total transmittance at this interface is $(.99855)^2 = .997$. When the medium is air,

$$R_{interface} = \left[\frac{1.5-1.0}{1.5+1.0}\right]^2 = .04.$$

Thus, for air, the total transmittance at this interface is $(.96)^2 = .9216$. The ratio of the intensity of the instrument readings with air as the medium compared to iso-octane as the medium is $\frac{.9216}{.997} = .9243$. Therefore, instrument readings taken with iso-octane as the medium must be multiplied by .9243 before they can be compared to readings taken with air as the medium (including the reference mirror in particular). By a similar calculation, readings taken with benzene as the medium (refractive index 1.5) must be multiplied by .9216. The experimentally observed ratio of reference mirror readings taken in air

to those taken in iso-octane is .91; the ratio of air to benzene readings is .90. However, these experimental values are not corrected for any changes in reflectivity of the aluminum reference mirror which occur when it is immersed in iso-octane or benzene.

F. Potential Sources of Error

1. Systematic

An apparent difference in reflectivity can be noticed when different sources are used. This can happen when a change is made from the tungsten lamp to the deuterium arc when going from the visible spectrum to the ultraviolet. One source of this difficulty is room light. The effect is that the spectrum taken with the lower intensity source appears to have a higher reflectivity than its true value. The reason that it appears higher is that both the signal from the standard mirror and the signal from the crystal have a constant room light signal added to them. Since the crystal reflectivity is less than the mirror reflectivity, the constant room light signal is a greater percent of the total observed signal. Thus, when the ratio of crystal signal to mirror signal is taken, the resulting value is too high. A stray light measurement made with nothing in the focal position is extremely sensitive to room light and must always be made in a darkened room. Therefore, it cannot be used to correct for the effect of

room light. When measurements of the standard mirror are being made with an intense light source, the effect of room light is negligible. In other cases the room must be darkened or the microscope stage area shielded.

Another way in which discrepancies in reflectance can arise when sources are changed is due to instrumental stray light in combination with the spectral response of the instrument. Consider the region of the spectrum near 375 nm. This is the region where the change from tungsten source to deuterium source is usually made. Both sources emit at relatively low intensity in this region. The peak intensity of the tungsten emission is in the visible region, and the peak intensity of the deuterium is in the ultraviolet region. Consider a crystal which has its reflectance peaked in the ultraviolet region. When the reflectance at 375 nm is measured with the deuterium source, the stray light is composed principally of ultraviolet light which the crystal reflects strongly. Thus, the apparent reflectance would be too high. However, when the tungsten source is used, the stray light is predominately visible radiation which the crystal reflects weakly. The situation can be very complex. The overall spectral response of the instrument should be considered rather than the spectral characteristics of the sources. The effect becomes more pronounced in regions of the spectrum which are removed from the apparent source spectrum peak. The best

solution to this problem would be to reduce the system stray light by using a double monochromator configuration.

Other potential sources of systematic errors include imperfections in crystal surfaces, misalignment of the crystal, improper calibration of reference mirror, crystal fluorescence, and nonlinear photomultiplier tube response. Additional errors arise when a liquid medium is used. The index of refraction of a liquid is generally a function of temperature and wavelength; if the wrong value is used for the index of refraction of the liquid, the calculated correction factor (discussed above) will be in error, thus producing an error in the reflectance.

2. Random

The principal source of random error is drift in instrument response. In a single beam system, there is a time interval on the order of a few minutes between measurement of the sample and the reference standard. A drift in response during the time it takes to make both measurements produces an error in the observed reflectance. After 30 minutes warmup, drift is generally less than one percent. This source of error could be removed by using a dual beam system with one beam monitoring the reference standard. Reading error and noise amount to ±.1 unit of the chart paper (100 divisions full scale); this combined with drift produces a typical error of ±1.% in each instrument reading.

The reflectance of the crystal is calculated as

$$R = \left[\frac{I_x - I_b}{I_m - I_b}\right] F \ , \qquad \text{eq. 3-3}$$

where I_x = intensity reading for the crystal,

I_m = intensity reading for reference mirror,

I_b = intensity reading of stray light, and

F = reflectance of reference mirror. The maximum error in R is approximated by differentiating eq. 3-3 and substituting the maximum error in each intensity reading as the differential increment. When using the fluorite objective, I_b is about .036 I_m; when using the reflecting objective, I_b is about .003 I_m. Thus, for the purpose of estimating ΔR, the values of I_b and ΔI_b are negligible in comparison to I_m. Substituting I_m for $I_m - I_b$ in eq. 3-3 gives

$$R = \frac{F(I_x - I_b)}{I_m} = \frac{FI_x}{I_m} - \frac{FI_b}{I_m} \ . \qquad \text{eq. 3-4}$$

Then,

$$\Delta R = \frac{FI_m\Delta I_x - FI_x\Delta I_m}{I_m^2} - \frac{FI_m\Delta I_b - FI_b\Delta I_m}{I_m^2}$$

and

$$\Delta R = \frac{F(\Delta I_x - \Delta I_b)}{I_m} - \frac{F\Delta I_m(I_x - I_b)}{I_m^2} .$$

In order to obtain the maximum value for ΔR, negative values are assumed for ΔI_b and ΔI_m, so that

$$\Delta R = \frac{F(\Delta I_x + \Delta I_b)}{I_m} + \frac{F\Delta I_m(I_x - I_b)}{I_m^2}. \qquad \text{eq. 3-5}$$

Since the maximum error in the instrument readings is about $\pm 1.\%$, $\Delta I_x = .01\ I_x$, $\Delta I_b = .01\ I_b$, and $\Delta I_m = .01\ I_m$.

Substituting these values into eq. 3-5 gives

$$\Delta R = \frac{.01\ F(I_x + I_b)}{I_m} + \frac{.01\ F\ (I_x - I_b)}{I_m}$$

which may be rewritten as

$$\Delta R = \frac{.02\ F(I_x - I_b)}{I_m} + \frac{.02\ FI_b}{I_m}.$$

Substituting from eq. 3-4 and setting $F = .9$

$$\Delta R = \pm \left[.02R + \frac{.018\ I_b}{I_m} \right]. \qquad \text{eq. 3-6}$$

For the fluorite objective, $I_b = .036\ I_m$, and

$$\Delta R = \pm(.02R + .0007). \qquad \text{eq. 3-7}$$

For the reflecting objective, $I_b = .003\ I_m$, and

$$\Delta R = \pm(.02 + .00005). \qquad \text{eq. 3-8}$$

Equations 3-7 and 3-8 can be used to estimate the maximum error in measured reflectances when using the fluorite or reflecting objectives respectively. The equations show that the reflecting objective is preferred for measuring reflectances less than .1. For reflectances greater than .1, the maximum error is ±2% of the reflectance.

G. Spectra

For the work reported herein, the best quality crystals were defined as those which when examined with a microscope showed no visible imperfections of the area of the surface to be used for measurements and which gave the maximum reflection intensity that was reproducible among several crystals.

The Rmax direction was determined by monitoring the intensity of light reflected by the crystal at a specified wavelength as the crystal was rotated (by rotating the circular stage). The orientation which produced the maximum intensity was defined as the Rmax direction. The Rmin direction was defined as 90° from the Rmax direction.

The following spectra of face 3 of BDP^{11} were measured with the instrument and techniques described in sections III A, B, and E. Their theoretical implications will be discussed in chapter IV. Other spectra obtained with this instrument and not reported elsewhere are presented in appendix A.

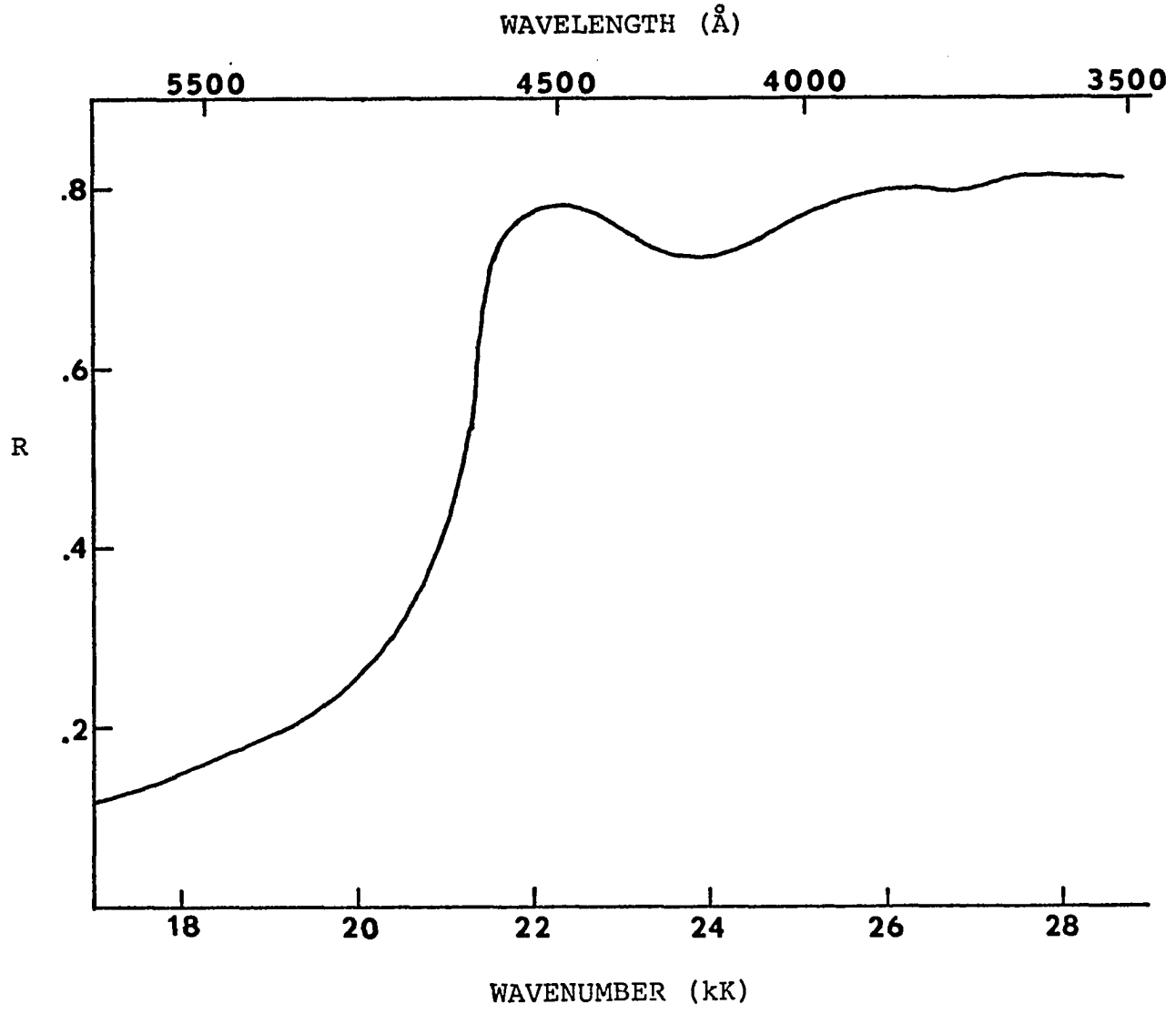

Figure 3-2. Polarized reflection spectrum for Rmax (4560 Å) for face 3 of BDP in iso-octane.

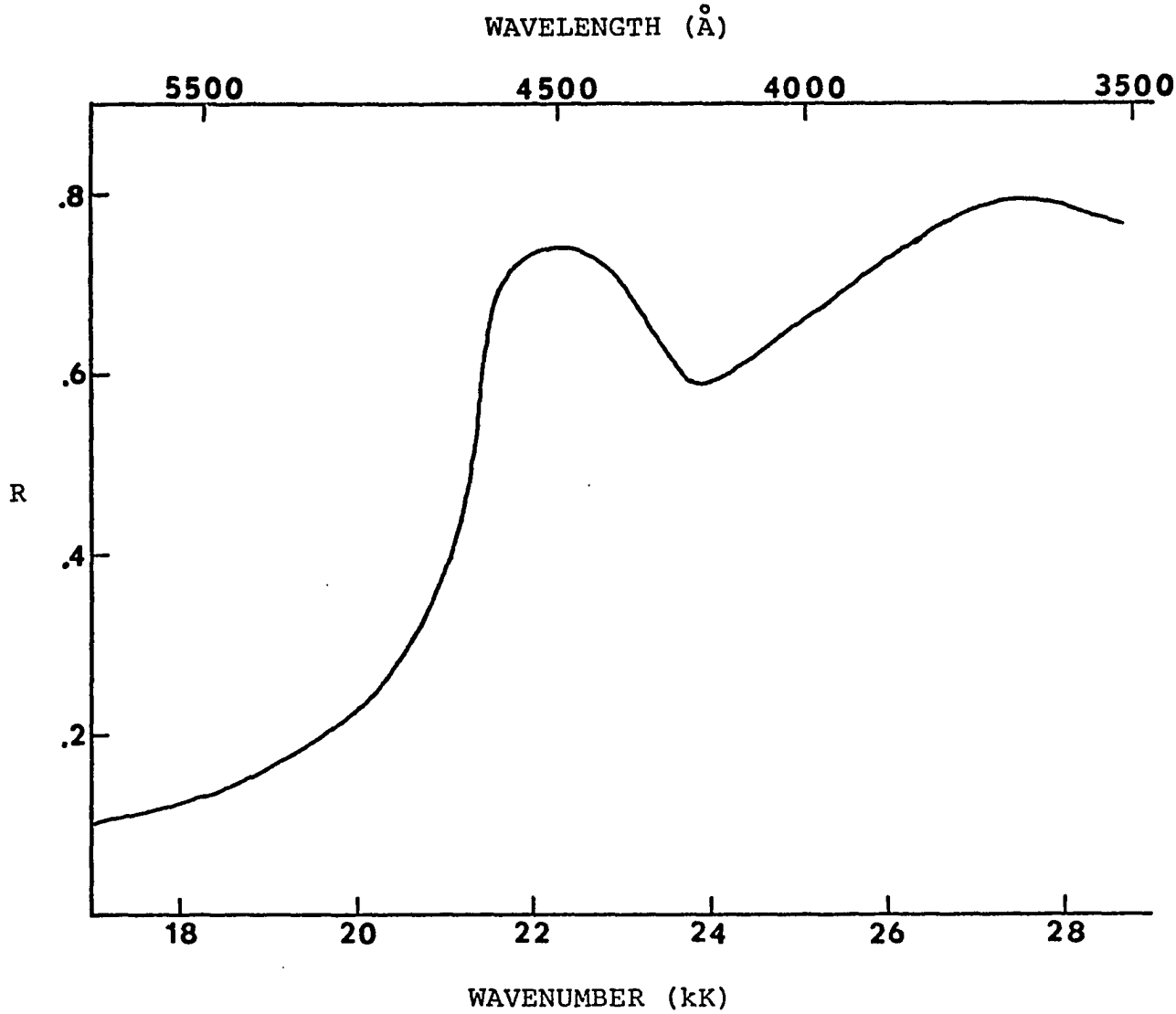

Figure 3-3. Polarized reflection spectrum for Rmax (4560 Å for face 3 of BDP in benzene.

CHAPTER IV

DETERMINATION OF OPTICAL CONSTANTS

A. Introduction

The problem of obtaining reliable optical constants from measurements which can be made with the reflectance microspectrophotometer described in chapter III is considered in this chapter. Since the normal incidence Kramers-Kronig approach is so attractive experimentally (requiring only one reflectance measurement, normal incidence, and permitting small crystals), it has been reexamined thoroughly as a means of obtaining optical constants. The general theory is presented in section B.1. An inherent difficulty with this method is the problem of how to properly account for the effect of the unobserved spectral wings. Various methods for solving the "wing" problem are discussed in section B.2. In particular, an effort was made to find a method which is convenient, accurate, and generally applicable. It is found that all of the methods inevitably give rise to adjustable parameters in the calculations. Furthermore, large changes in the derived absorption spectra can occur when small changes

are made in the various adjustable parameters. Various techniques for determining the adjustable parameters are considered in section B.3. The conclusion reached from these considerations is that in the UV-visible spectral region there is no generally applicable method of explicitly determining the adjustable parameters given only the normal incidence reflectance spectrum. Thus, it is desirable to measure one of the optical constants by an independent method at a number of wavelengths equal to the number of adjustable parameters if the Kramers-Kronig method is to be used.

Possibilities of determining optical constants from measurements made with the spectrophotometer described in chapter III without recourse to the Kramers-Kronig analysis were considered. Non-normal incidence measurements are considered in section C; transmission measurements are discussed in section D. Normal incidence reflectance measurements in mediums of different refractive index are considered in section E. A new technique, using liquids as the different mediums, is formulated. The theory, a discussion of errors, and experimental data verifying the technique are presented. This method is particularly attractive because of its simplicity as well as its general applicability. Although for some systems it becomes error prone in certain spectral regions, it can always be used as an independent measurement for the explicit determination of the adjustable parameters in the Kramers-Kronig analysis.

B. Kramers-Kronig Analysis

1. Theory

Only the case of normal incidence reflection is considered. The following development is adapted from Ditchburn.[1] For light incident from a vacuum on an absorbing medium, the index of refraction and the amplitude of the reflected wave are complex. Thus, $\tilde{n}=n-ik$, where $\tilde{n}$ is the complex index of refraction, n is the real part of the complex index, and k is the extinction coefficient (or imaginary part of the complex index). At normal incidence,

$$\tilde{r} = re^{i\theta} = \frac{n-ik-1}{n-ik+1} \qquad \text{eq. 4-1}$$

where $\tilde{r}$ is the complex amplitude of the reflected wave, θ is the phase angle, and r is the real part of the complex amplitude.

The molar extinction coefficient, ε, may be calculated from the known value of k;

$$\varepsilon = \frac{-4\pi k}{2.303\lambda M} \qquad \text{eq. 4-2}$$

where M is the molar concentration, and λ is the wavelength.

The intensity of the reflected wave at normal incidence is given by the Fresnel equation,

$$R = \tilde{r}\cdot\tilde{r}^* = r^2 = \frac{(n-1)^2 + k^2}{(n+1)^2 + k^2} . \qquad \text{eq. 4-3}$$

By separating the real and imaginary parts of equation 4-1, it may be shown that

$$n = \frac{1-r^2}{1+r^2 - 2r(\cos\theta)} \qquad \text{eq. 4-4}$$

and

$$k = \frac{-2r(\sin\theta)}{1+r^2 - 2r(\cos\theta)} . \qquad \text{eq. 4-5}$$

Thus, if both R and θ are known at a particular frequency, the value of n and k can be calculated at that frequency from eq. 4-4 and eq. 4-5.

θ at each frequency may be calculated if the complete reflection spectrum is known. R and θ are not independent but are connected by a dispersion relation (Kramers-Kronig transformation) which may be written

$$\theta(\omega_i) = \frac{\omega_i}{\pi} \int_0^\infty \frac{\ln R(\omega) - \ln R(\omega_i)}{\omega_i^2 - \omega^2} d\omega \qquad \text{eq. 4-6}$$

where ω is the circular frequency, $\theta(\omega_i)$ indicates the phase when ω has the value ω_i, etc.[4] Although this mathematical transformation is exact, eq. 4-6 cannot be evaluated exactly due to a lack of knowledge of the behavior of $R(\omega)$

outside the observable frequency range. The evaluation of $\theta(\omega_i)$ from eq. 4-6 when $R(\omega)$ is only known explicitly over a finite region is a fundamental problem of normal incidence reflection spectroscopy known as the wing problem. The unobserved "wings" of the spectrum strongly influence the results of the Kramers-Kronig calculations. Small changes in the values assigned to the wings can cause the calculated values of the molar extinction coefficient to vary considerably and even become negative.

2. Approaches to the Wing Problem

The general approach is to measure $R(\omega)$ over a region of the spectrum from $\omega = \omega_a$ to $\omega = \omega_b$. Equation 4-6 is then broken into three integrals as follows:

$$\theta(\omega_i) = \theta_L(\omega_i)+\theta_M(\omega_i)+\theta_H(\omega_i) \qquad \text{eq. 4-7}$$

where

$$\theta_L(\omega_i) = \frac{\omega_i}{\pi} \int_0^{\omega_a} \frac{\ln R(\omega)-\ln R(\omega_i)}{\omega_i^2-\omega^2}\, d\omega \,, \qquad \text{eq. 4-8}$$

$$\theta_M(\omega_i) = \frac{\omega_i}{\pi} \int_{\omega_a}^{\omega_b} \frac{\ln R(\omega)-\ln R(\omega_i)}{\omega_i^2-\omega^2}\, d\omega \,, \qquad \text{eq. 4-9}$$

$$\theta_H(\omega_i) = \frac{\omega_i}{\pi} \int_{\omega_b}^{\infty} \frac{\ln R(\omega) - \ln R(\omega_i)}{\omega_i^2 - \omega^2} \, d\omega. \qquad \text{eq. 4-10}$$

$\theta_M(\omega_i)$ can be evaluated explicitly using either Simpson's rule or the trapezoid rule for numerical integration. Some methods of approximating the effects of the wings, $\theta_L(\omega_i)$ and $\theta_H(\omega_i)$, is then employed. Various extrapolation procedures have been devised for calculating the effect of the wings. An argument central to most techniques is that the resonance denominator in eq. 4-6 reduces the contribution from regions of the spectrum sufficiently removed from the region being studied.

One of the simplest methods[14] is to extend the region of measured reflectance far enough away from the peak so that R is experimentally constant. If R is then assumed to stay at this value throughout the unobserved regions, eq. 4-8 and 4-10 can be integrated analytically with the following results:

$$\theta_L(\omega_i) = \frac{1}{2\pi} \ln \frac{R(\omega_a)}{R(\omega_i)} \ln \frac{(\omega_i + \omega_a)}{(\omega_i - \omega_a)} \qquad \text{eq. 4-11}$$

and

$$\theta_H(\omega_i) = \frac{1}{2\pi} \ln \frac{R(\omega_b)}{R(\omega_i)} \ln \frac{(\omega_b - \omega_i)}{(\omega_b + \omega_i)} \; . \qquad \text{eq. 4-12}$$

In general this approximation is poor, often yielding negative values and serious distortions of k.[4] In practice the values of eq. 4-11 and 4-12 are very sensitive to the value of $R(\omega_a)$ and $R(\omega_b)$ at the endpoints of the observable region. The value of $\theta(\omega_i)$ is in fact a function of the endpoints of the observable region if R is not perfectly constant.

The reflection spectrum of face 3 of BDP and the resulting calculated extinction coefficients as reported by Neely[11] are shown in Figures 4-1 and 4-2, respectively. This absorption spectrum (which was calculated using the "constant R" approximation) agrees well with the absorption in the 4350-3330 Å region and the absorption peak (average ε of 1.5×10^5) found by Fratini[19] for thin film BDP absorption measurements. The spectrum is also consistent with other theoretical calculations reported by Neely.[11] Thus, the set of data reported by Neely for face 3 of BDP was felt to be the most reliable available for BDP and was initially selected as the data set for testing various approximations used in the Kramers-Kronig calculations. It may be noted that the optical constants reported by Neely[11] for the 4000-3500 Å and the 5850-5000 Å ranges were subsequently confirmed by independent measurements reported in section IV.E.3.

Figure 4-3 presents the results of applying the "constant R" approach to the test data in Figure 4-1 using

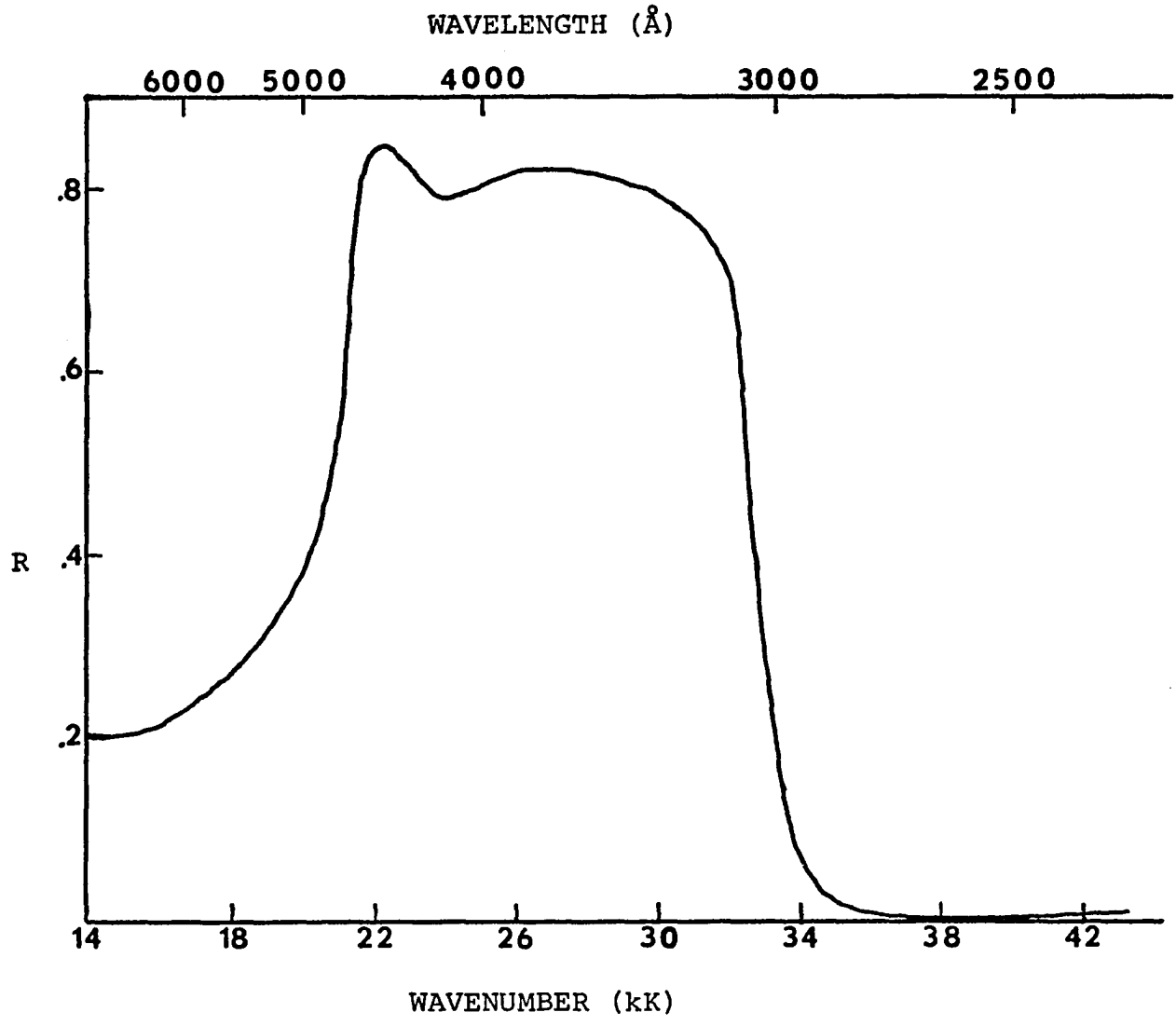

Figure 4-1. Polarized reflection spectrum for face 3 of BDP as reported by Neely.[11]

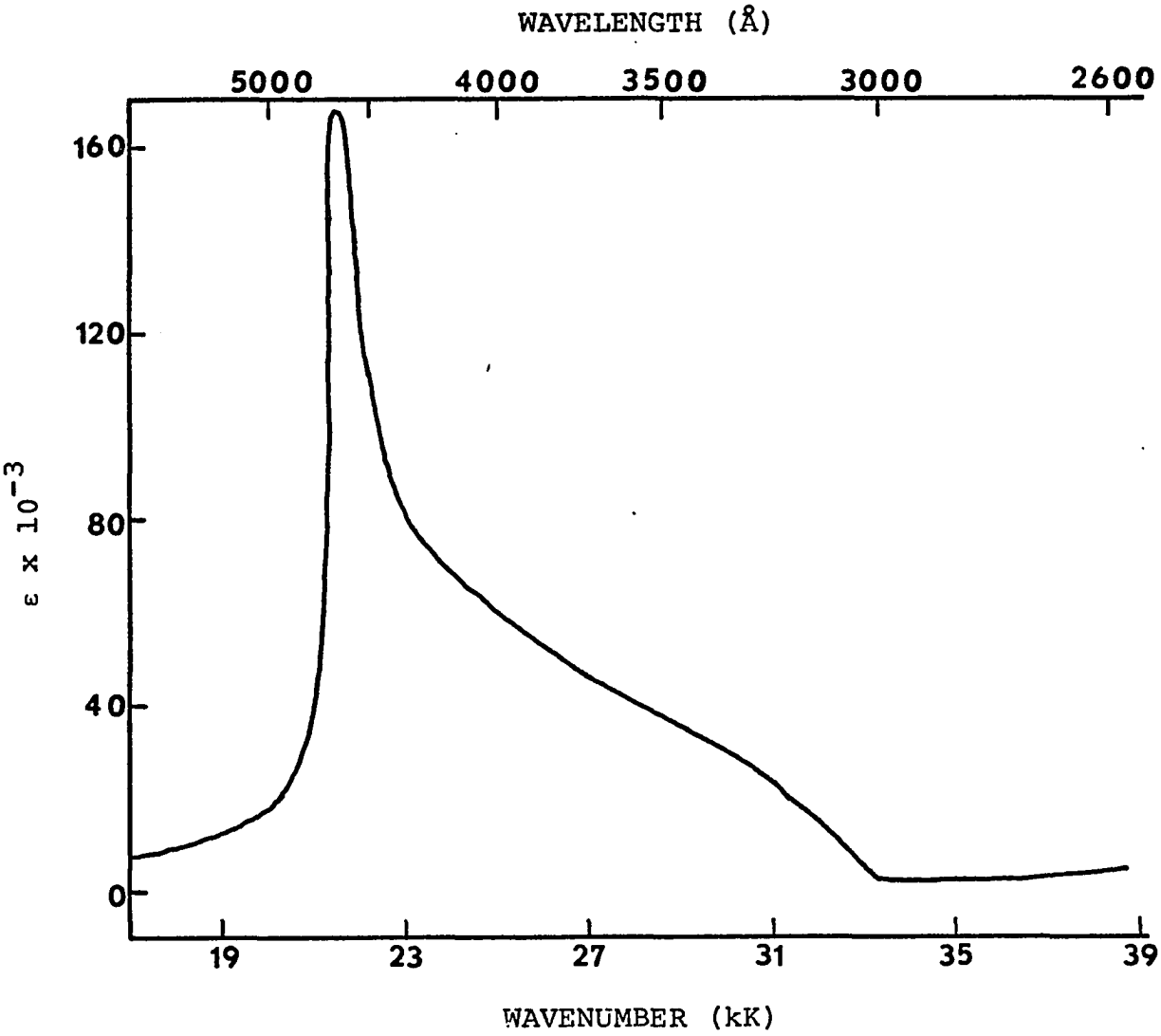

Figure 4-2. Polarized absorption spectrum for face 3 of BDP calculated using constant R approximation (as reported by Neely).[11] Integration limits 7194 to 2310 Å.

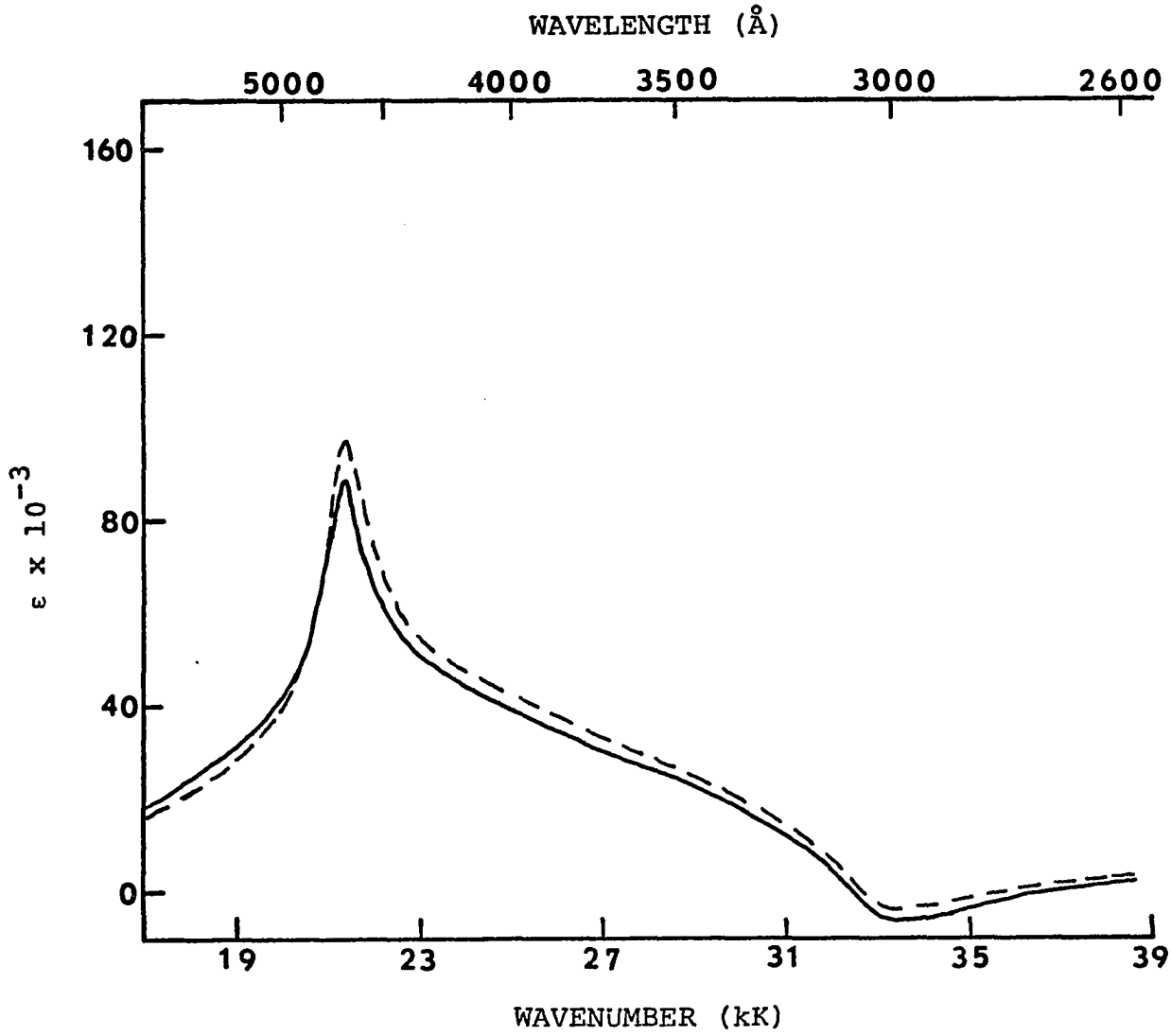

Figure 4-3. Polarized absorption spectrum for face 3 of BDP calculated using constant R approximation. Solid line for integration limits 6410 to 2600 Å; dashed line for integration limits 6473 to 2708 Å.

two different wavelength ranges for the "observed" region. Considerable variation in intensities and slopes is seen to occur for apparently modest truncations of the experimental data. The peak location itself is less dramatically affected, but does exhibit a distinct shift of about 0.2 kK (or 40 Å).

Obviously, one of the criteria which a method for calculating the wings must satisfy is that $\theta(\omega_i)$ should be independent of the endpoints chosen for the observable region. We have attempted to improve the "constant R" method of calculation by including adjustable scaling factors in eq. 4-11 and eq. 4-12. The resulting equations are:

$$\theta_L(\omega_i) = A \frac{1}{2\pi} \ln\frac{R(\omega_a)}{R(\omega_i)} \ln\frac{\omega_i+\omega_a}{\omega_i-\omega_a} \qquad \text{eq. 4-13}$$

and

$$\theta_H(\omega_i) = B \frac{1}{2\pi} \ln\frac{R(\omega_b)}{R(\omega_i)} \ln\frac{\omega_b-\omega_i}{\omega_b+\omega_i} . \qquad \text{eq. 4-14}$$

The constants A and B can be determined if $\theta(\omega_i)$ is known at two frequencies in the observed region of the spectrum. An example calculated from the BDP reflection spectrum (Figure 4-1) is shown in Figure 4-4. The values of $\theta(\omega_i)$ were selected from the Kramers-Kronig output associated

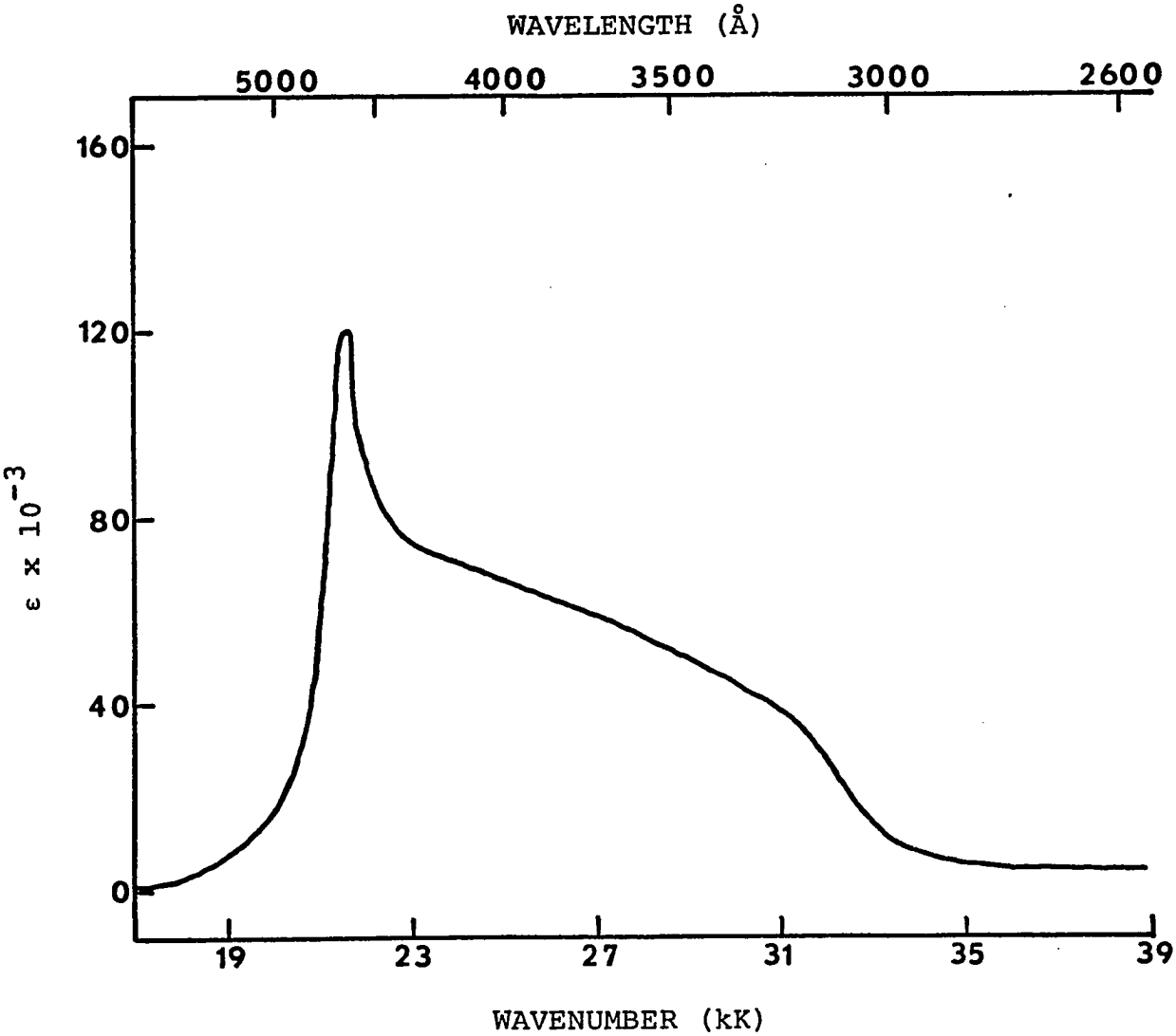

Figure 4-4. Polarized absorption spectrum for face 3 of BDP calculated using scaled wing method. Integration limits 6410 to 2600 Å. Theta defined as 0.1005 at 4952 Å and 1.5414 at 2605 Å, corresponding to figure 4-2.

with the absorption spectrum in Figure 4-2.[11] Specifically, θ was defined to be 0.1005 at 4952 Å and 1.5414 at 2605 Å. Some improvement in shape and overall intensity has occurred compared to the constant R calculations shown in Figure 4-3. However, there is still a reduction of the extinction coefficient of almost 30% (compared to Figure 4-2). The calculated values of $\theta(\omega_i)$ still depend on the chosen endpoints for the observable region. Thus, the "scaled wing method," which is an extension of the "constant R" approximation, still leaves much to be desired in terms of accuracy and reliability.

Another method[15] of handling the wing problem is to guess trial reflection curves for the inaccessible spectral regions and then vary these trial functions until the computed absorption is essentially zero through the known transparent spectral region. Forcing the computed absorption to go to zero in a known transparent region of the spectrum, called "k=0 in the wings" approximation, is a frequently used technique[7,9,15,23] of attempting to determine adjustable parameters and is discussed in section IV. B.3.c. The accuracy of the guessed reflection curve method is questionable. Its chief value is that it demonstrates that the calculated absorption curve is fairly insensitive to the shape of the reflectance curve in the unobserved region.

In the method by Andermann et al.[4] artificial wings are generated based on an undamped harmonic-oscillator model of an absorption band. There are several variable parameters which are adjusted to force the wings of the Kramers-Kronig

calculation to fall off as a Cauchy curve. This method is capable of better accuracy than the methods discussed above, but accuracy depends on how well the actual spectrum resembles a Cauchy curve. It is complicated to use, and some degree of freedom in picking values for the adjustable parameters is still allowed. This method might be improved by measuring the optical constants near the wings by an independent method such as the one described in section IV. E. and then forcing the Kramers-Kronig output to fall off along the measured curve rather than a Cauchy curve.

All of the methods discussed above are based on assuming a shape for the reflectance spectrum in the unobserved regions, and then evaluating $\theta_L(\omega_i)$ and $\theta_H(\omega_i)$ explicitly using Simpson's rule, etc. For each method in order to evaluate $\theta_H(\omega_i)$, it is necessary to assume that the reflectance has a constant value beyond an arbitrary high spectral frequency. A more generalized approach to the problem is to attempt to find a value for $\theta_L(\omega_i)$ and $\theta_H(\omega_i)$ without assuming anything about the behavior of the reflectance in the unobserved region. One way of doing this is to apply the mean value theorem to the integrals in eq. 4-8 and eq. 4-10. The simple form of the mean value theorem may be written as

$$\int_a^b f(\chi)d\chi = (b-a)f(C). \qquad \text{eq. 4-15}$$

We applied this relationship to eq. 4-8 to obtain

$$\theta_L(\omega_i) = \frac{\omega_a \omega_i}{\pi} \frac{\ln R(C) - \ln R(\omega_i)}{\omega_i^2 - C^2} . \qquad \text{eq. 4-16}$$

If the value of C which satisfies this equation is approximately independent of ω_i over the region of interest, eq. 4-16 could be used to evaluate $\theta_L(\omega_i)$ over this region once the values of C and R(C) have been determined. The simple mean value theorem cannot be applied to eq. 4-10 directly because the factor (b-a) in eq. 4-15 would be undefined. One way to avoid this difficulty would be to use the simple mean value theorem over some arbitrary interval and then assume that $R(\omega)$ remains constant beyond the chosen interval. Thus, eq. 4-10 would be modified to give

$$\theta_H(\omega_i) = \frac{\omega_i}{\pi} \int_{\omega_b}^{\omega_c} \frac{\ln R(\omega) - \ln R(\omega_i)}{\omega_i^2 - \omega^2} d\omega +$$

eq. 4-17

$$\frac{\omega_i}{\pi} \int_{\omega_c}^{\infty} \frac{\ln R(\omega_c) - \ln R(\omega_i)}{\omega_i^2 - \omega^2} d\omega .$$

Applying the simple mean value theorem to the first term

on the right hand side of eq. 4-17 and integrating the second term explicitly gives

$$\theta_H(\omega_i) = (\omega_c-\omega_b)\ \frac{\omega_i}{\pi}\ \frac{\ln R(d)-\ln R(\omega_i)}{\omega_i^2-d^2}\ +$$

eq. 4-18

$$\frac{1}{2\pi}\ln\frac{R(\omega_c)}{R(\omega_i)}\ln\frac{\omega_c-\omega_i}{\omega_c+\omega_i}.$$

The values of d, $R(d)$, $R(\omega_c)$, and ω_c would have to be determined to use eq. 4-18; the value of d would have to to be approximately independent of ω_i over the region of interest. The value of ω_c could perhaps simply be increased until no change in the calculated value of $\theta_H(\omega_i)$ is observed for further increases in ω_c. In order to apply eq. 4-16 and 4-18 to calculate $\theta(\omega_i)$, a total of six constants must be determined. This would require knowing the value of $\theta(\omega_i)$ at six different frequencies in the observed region.

The same general approach was used by Roessler[7] with the extended mean value theorem rather than the simple mean value theorem. According to the extended mean value theorem, if $\rho(\chi)$ is > 0, then

$$\int_a^b f(\chi)\rho(\chi)d\chi = f(c)\int_a^b \rho(\chi)d\chi. \qquad \text{eq. 4-19}$$

This may be applied to eq. 4-8 by defining

$$\rho(\chi) \equiv \frac{1}{\omega_i^2-\omega^2} \quad \text{and} \quad f(\chi) \equiv \ln R(\omega)-\ln R(\omega_i).$$

For $\theta_L(\omega_i)$ it is always true that $\omega_i > \omega$ hence $\rho(\chi) > 0$ as required. Then,

$$\theta_L(\omega_i) = \frac{\omega_i}{\pi}\left[\ln R(C)-\ln R(\omega_i)\right]\int_0^{\omega} \frac{d\omega}{\omega_i^2-\omega^2},$$

and

$$\theta_L(\omega_i) = \frac{1}{2\pi}\ln\frac{R(C)}{R(\omega_i)}\ln\frac{\omega_i+\omega_a}{\omega_i-\omega_a} \qquad \text{eq. 4-20}$$

Similarly for eq. 4-10,

$$\rho(\chi) \equiv \frac{1}{\omega^2-\omega_i^2} \qquad \text{and} \qquad f(\chi) \equiv \ln R(\omega_i)-\ln R(\omega).$$

For the high frequency wing $\omega > \omega_i$ hence $\rho(\chi) > 0$.

Then,

$$\theta_H(\omega_i) = \frac{\omega_i}{\pi} \ln \frac{R(\omega_i)}{R(d)} \int_{\omega}^{\infty} \frac{d\omega}{\omega^2 - \omega_i^2}$$

and

$$\theta_H(\omega_i) = \frac{1}{2\pi} \ln \frac{R(d)}{R(\omega_i)} \ln \frac{\omega_2 - \omega_b}{\omega_2 + \omega_b} \quad . \qquad \text{eq. 4-21}$$

These equations were derived independently, however, with a change of notation and form they are equivalent to those published by Roessler.[7,9]

Notice that eq. 4-20 is identical in form to eq. 4-11 and eq. 4-21 is identical in form to eq. 4-12, except that $R(\omega_a)$ is replaced by R(c) and $R(\omega_b)$ is replaced by R(d) respectively. In fact, eq. 4-20 and 4-21 could have been derived from 4-11 and 4-12 by putting scaling factors with $R(\omega_a)$ and $R(\omega_b)$. This method is thus equivalent to using the constant $R(\omega)$ approximation with the exception that $R(\omega)$ is not assumed to remain at the value it has at the endpoints of the observable region, but rather its effective value (which is a function of the endpoints) is determined from known values of $\theta(\omega_i)$. Scaling the value of $R(\omega_a)$ and $R(\omega_b)$ is not equivalent to scaling the entire wing term which led to eq. 4-13 and 4-14. Roessler's method is also equivalent to the method of Schatz et al.[23] who arbitrarily let lnR(c) and lnR(d) be adjustable parameters. Both Roessler and Schatz then use the "k=0 in the wings" approximation to evaluate the parameters (see section IV. 3. c. for a discussion of this approximation).

As for the accuracy of using the extended mean value theorem, note that eq. 4-8 may be separated into two terms as follows:

$$\theta_L(\omega_i) = \frac{\omega_i}{\pi} \int_0^{\omega_a} \frac{\ln R(\omega)}{\omega_i^2-\omega^2} d\omega - \frac{\omega_i}{\pi} \int_0^{\omega_a} \frac{\ln R(\omega_i)}{\omega_i^2-\omega^2} d\omega.$$

The second term may be integrated analytically to give

$$- \frac{1}{2\pi} \ln R(\omega_i) \ln \frac{(\omega_i+\omega_a)}{(\omega_i-\omega_a)} .$$

Thus, it is only necessary to apply the extended mean value theorem to the first term which yields

$$\frac{1}{2\pi} \ln R(c) \ln \frac{(\omega_i+\omega_a)}{(\omega_i-\omega_a)} .$$

When this is combined with the second term, the result is

$$\theta_L(\omega_i) = \frac{1}{2\pi} \ln \frac{R(c)}{R(\omega_i)} \ln \frac{(\omega_i+\omega_a)}{(\omega_i-\omega_a)} .$$

This is identical to eq. 4-20 which was obtained by applying the extended mean value theorem to both terms in eq. 4-8. Thus, for the $R(\omega_i)$ term, there is no error at all in using the extended mean value theorem. By a similar calculation, it can be shown that for the $R(\omega_i)$

term in eq. 4-10, there is no error in using the extended mean value theorem. This is not true for the simple mean value theorem.

Eq. 4-20 and 4-21 each have only one constant to be determined. Thus, in order to use these equations it is necessary to know the value of $\theta(\omega_i)$ at only two frequencies in the observable region, which is a considerable advantage over other methods. For these equations to be useful R(c) and R(d) must be approximately independent of ω_i over the region of interest. A trial calculation using the BDP spectrum (Figure 4-1) is shown in Figure 4-5. As was done for the calculations shown in Figure 4-4, the values of $\theta(\omega_i)$ were selected from the Kramers-Kronig output associated with the absorption spectrum in Figure 4-2. Again, θ was defined to be 0.1005 at 4952 Å and 1.5414 at 2605 Å. The agreement with the literature spectrum in Figure 4-2 is very good. The intensities and slopes of the two curves are very similar over all of the observed region. The wavelengths of the absorption maxima are the same, and there is less than 5% difference in the maximum intensities. Thus, the present application of the extended mean value theorem provides accurate results which are clearly much less sensitive to endpoint selection than the alternative methods presented earlier. This method is particularly attractive because of the simplicity as well as the accuracy of the approach. The simplicity lies in

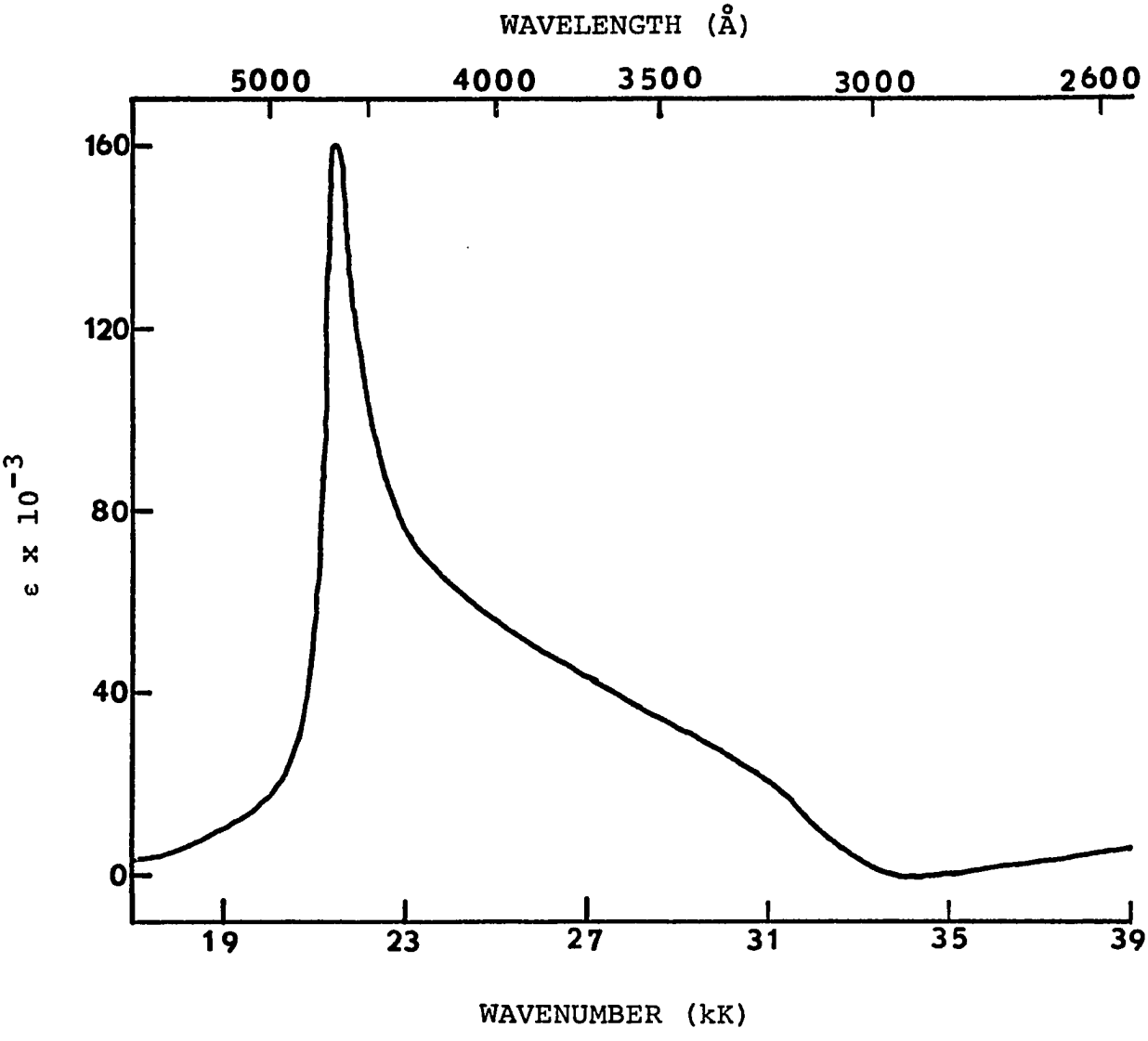

Figure 4-5. Polarized absorption spectrum for face 3 of BDP calculated using the extended mean value theorem approximation. Integration limits 6410 to 2600 Å. Theta defined as 0.1005 at 4952 Å and 1.5414 at 2605 Å, corresponding to figure 4-2.

the form, only two constants to determine, as well as in the ease of application. The accuracy is so good that it is a useful, general method for the determination of optical constants from reflectance data provided that the constants can be accurately determined.

3. Comments on the Determination of Adjustable Parameters

a. Introduction

All of the available methods for treating the wing problem give rise to "constants" in the calculation. Since the values of the "constants" are unknown, they are effectively, if not explicitly, adjustable parameters. If the constants are not uniquely determined, then the results of the Kramers-Kronig calculations are questionable. If θ, n or k were known at a number of frequencies equal to the number of parameters to be determined in the observable region, the constants would be uniquely determined from eq. 4-4, 4-5, or 4-6. However, the necessary values of θ, n, or k are usually not known. Since it is inconvenient to measure them independently, several possibilities were considered for determining the constants uniquely without making experimental measurements other than the normal incidence reflectance spectrum. These

possibilities are discussed in the following sections b, c and d.

b. Physical Restrictions

Restrictions on permissible values of θ will restrict the permissible values of the adjustable parameters. A physical restriction is that $0 \leq \theta \leq \pi$.[5] This can be seen by considering the relation between k, r, and θ (eq. 4-5) and the relation between k and the molar extinction coefficient, ε (eq. 4-2). Since the molar extinction coefficient $\varepsilon \geq 0$, this implies $k \leq 0$. From eq. 4-5, $k \leq 0$ if $\sin\theta \geq 0$, since $0 \leq r < 1$ and since the denominator term > 0. That the denominator term $(1 + r^2 - 2r\cos\theta) > 0$ may be seen by the following considerations. If $\pi/2 \leq \theta \leq 3\pi/2$ then, $\cos\theta \leq 0$ and the denominator is positive. If $0 \leq \theta \leq \pi/2$ then $1 \geq \cos\theta \geq 0$. The maximum value of the negative term is -2r. The denominator then is given by $1 + r^2 = 2r = (1-r)^2$. Since $0 \leq r < 1$ at normal incidence, the denominator is always > 0. Thus, $\sin\theta \geq 0$, which implies $0 \leq \theta \leq \pi$.

Although physical restrictions limit the values of the parameters, they do not uniquely determine the values.

c. Approximations

A frequently used method[7,9,15,23] of determining adjustable parameters is to assume that k=0 in the wings of the absorption band (i.e., known transparent regions). Roessler[7,9] specifically assumes that $\theta=0$, however, from eq. 4-5 it can be seen that this assumption automatically implies that k=0 (if $r\neq 0$). Also, from eq. 4-5 it can be seen that if k=0, then $\theta=0$ or π, which is the assumption used by Schatz et al.[23] The chief limitation of this method is that if a system has a broad absorption band (such as BDP), k may be greater than zero over all of the observable region.[4] Thus, an independent measurement of the absorption spectrum may be required to determine at what frequencies, if any, k=0. Another disadvantage of this method is that the values of the adjustable parameters are frequently quite sensitive to the measured value of the reflectance in the wings;[5] small values of R are difficult to measure accurately, thus making the method somewhat error prone.

A method sometimes used in the analysis of infrared spectra of certain systems is the assumption that n = 1 before the onset of the reflectance band.[5] From eq. 4-4

it can be seen that $n = 1$ implies $1 + r^2 - 2r\cos\theta = 1-r^2$. Thus, $r\cos\theta - r^2 = 0$ and $r(\cos\theta - r) = 0$. If $r \neq 0$, then $\cos\theta = r$. However, for the UV and visible region of the spectrum, n may not have the value of 1.0 even in the absence of absorption, and hence this is not a safe assumption for these regions.

It is clear then that any such approximations of the phase, extinction coefficient, or index or refraction will be inadequate for a general approach.

d. Reflectance Slope Implications

From the experimental data over the observable region not only $R(\omega_i)$ is determined, but also $\frac{\partial R}{\partial \omega}$. The possibility of using this information was considered. The only equation which directly relates R and θ is eq. 4-6. This equation may be differentiated with respect to ω_i to obtain the following:

$$\frac{\partial \theta(\omega_i)}{\partial \omega_i} = \frac{1}{\pi} \int_0^\infty \frac{\ln R(\omega) - \ln R(\omega_i)}{\omega_i^2 - \omega^2} d\omega +$$

$$\frac{\omega_i}{\pi}\int_0^\infty \frac{\ln R(\omega)\,d\omega}{\omega_i^2-\omega^2} - \frac{\omega_i}{\pi R(\omega_i)}\frac{\partial R(\omega_i)}{\partial \omega_i}\int_0^\infty \frac{d\omega}{\omega_i^2-\omega^2} - \qquad \text{eq. 4-22}$$

$$\frac{2\omega_i^2}{\pi}\int_0^\infty \frac{\ln R(\omega)}{(\omega_i^2-\omega^2)^2}\,d\omega + \frac{2\omega_i^2}{\pi}\int_0^\infty \frac{\ln R(\omega_i)\,d\omega}{(\omega_i^2-\omega^2)^2}\,.$$

If this equation could be evaluated and if $\theta(\omega_i)$ were known at some value of ω_i, then eq. 4-22 could be used to generate other values of θ in the neighborhood of the known value of $\theta(\omega_i)$. If $\theta(\omega_i)$ is known at ω_i, then all terms except the fourth in eq. 4-22 can be evaluated at ω_i. The integral in the fourth term is similar to the integral in the second term except that the denominator is squared. Perhaps this integral could be approximated by the mean value theorem, but that would generate two new constants to be determined. Also, eq. 4-22 is limited by the fact that θ must be known at some frequency from independent formation. The utility of this equation was not further explored.

The Fresnel equation (eq. 4-3) may be differentiated with respect to ω to give

$$\frac{\partial R}{\partial \omega} = \frac{4(n^2-1)\frac{\partial n}{\partial \omega} - 4k^2\frac{\partial n}{\partial \omega} + 8nk\frac{\partial k}{\partial \omega}}{[(n+1)^2+k^2]^2} . \qquad \text{eq. 4-23}$$

Both $\frac{\partial n}{\partial \omega}$ and $\frac{\partial k}{\partial \omega}$ would have to be known in order to solve the equation simultaneously with the Fresnel equation for the unique determination of n and k. Determination of $\frac{\partial k}{\partial \omega}$ implies a relation between n and $\frac{\partial n}{\partial \omega}$; similarly, determination of $\frac{\partial n}{\partial \omega}$ implies a relation between k and $\frac{\partial k}{\partial \omega}$. Therefore, eq. 4-23 may have some use for curve fitting in favorable cases where $\frac{\partial n}{\partial \omega}$ or $\frac{\partial k}{\partial \omega}$ can be determined. If eq. 4-4 is differentiated with respect to ω, the result is

$$\frac{\partial n}{\partial \omega} = \frac{2(r^2\cos\theta+\cos\theta-2r)\frac{\partial r}{\partial \omega} + 2(r^3\sin\theta-r\sin\theta)\frac{\partial \theta}{\partial \omega}}{(1+r^2-2r\cos\theta)^2} . \qquad \text{eq. 4-24}$$

Both r and $\frac{\partial r}{\partial \omega}$ are known in the observable region. If $\frac{\partial n}{\partial \omega}$ is known at any frequency in this region, then eq. 4-24 implies a relation between θ and $\frac{\partial \theta}{\partial \omega}$ which must be satisfied at that frequency.

If eq. 4-5 is differentiated with respect to ω, the result is

$$\frac{\partial k}{\partial \omega} = \frac{(2r^2\sin\theta-2\sin\theta)\frac{\partial r}{\partial \omega} + (4r^2-2r\cos\theta-2r^3\cos\theta)\frac{\partial \theta}{\partial \omega}}{(1+r^2-2r\cos\theta)^2} . \qquad \text{eq. 4-25}$$

If $\frac{\partial k}{\partial \omega}$ is known at any frequency in the observed region, then eq. 4-25 implies a relation between θ and $\frac{\partial \theta}{\partial \omega}$ at that frequency. In favorable cases, by doing a crude transmission experiment it may be possible to determine the frequency at which k is a maximum or minimum even though a good measured value of k cannot be obtained. At these frequencies, $\frac{\partial k}{\partial \omega} = 0$ can then be substituted in eq. 4-25 to obtain a relation between θ and $\frac{\partial \theta}{\partial \omega}$ for curve fitting purposes.

Equations 4-22 through 4-25 illustrate that information about $\frac{\partial R}{\partial \omega}$ (slope of the reflection spectrum) does not of itself place any restrictions on the adjustable parameters. With additional information such as $\frac{\partial n}{\partial \omega}$ or $\frac{\partial k}{\partial \omega}$ it implies certain relationships which could be used for curve fitting but not for unique determination of the parameters. Since $\frac{\partial n}{\partial \omega}$ or $\frac{\partial k}{\partial \omega}$ are not generally obtainable, these equations are of limited value.

From the considerations above, it does not appear possible to uniquely determine the adjustable parameters given only the normal incidence reflectance spectrum. In order to determine the parameters it is necessary to measure either n or k independently in the observable region at a number of wavelengths equal to the number of adjustable parameters. Sections IV. C, D, and E which follow, discuss techniques for accomplishing this using the reflectance microspectrophotometer and techniques described in chapter III.

C. Non-normal Incidence Reflection

If the reflectance is measured at two different angles of incidence (one of the angles may be zero, i.e., normal incidence), the values of n and k may be determined at that frequency. The major disadvantage of trying to couple the usual non-normal incidence method with the normal incidence method is that much larger crystal dimensions (at least ten-fold) are required for the former. This is a severe problem at optical frequencies. In the IR region where non-normal incidence methods are more common, crystal polishing techniques have been developed to produce the relatively large optically flat surfaces required. However, to be optically flat in the UV region requires at least a ten-fold greater perfection of the crystal surface, because the wavelengths are much shorter. Analogous polishing techniques for the UV visible region are not readily available. Growing a sufficiently perfect crystal large enough is a difficult task. Another disadvantage of this method is the requirement of a second spectrophotometer capable of measuring R at different angles of incidence. It may be possible to circumvent both of these disadvantages by using the normal incidence reflection microspectrophotometer to measure reflectance at a non-normal angle of incidence. This could be done by exploiting the convergent properties of the microscope objectives.

By placing a central aperture stop in the back of an objective, the incident light would be restricted to a cone of plane-polarized light. The angle of incidence is equal to the angle from the central axis of the cone to its edge. By also placing a second stop, consisting of a disk with a slot from edge to edge through its center, in an appropriate position in the optical path, the incident light could be further restricted to include only a vertical slice through the incident cone. When this stop was turned so that the length of the slot was parallel to the plane of polarization, the incident light would be polarized in the plane of incidence. Simply rotating the stop ninety degrees would produce light polarized perpendicular to the plane of incidence (the crystal would have to also be rotated ninety degrees to preserve the relative configuration of the crystal and the light beam). The major restriction of this technique is the relatively small angle of incidence attainable, i.e., about 27 degrees with the 50X reflecting objective. The method is most sensitive when using light polarized with the electric vector parallel to the plane of incidence.[2] Using light with this polarization incident at 27 degrees, the method will still be very insensitive if either n or $k > 1$.[2] Although 27 degrees would be too small an angle for most of the spectrum, it would be sufficient over regions of the spectrum where n and $k < 1$. This appears to be a promising method of deter-

mining the adjustable parameters in the Kramers-Kronig analysis. A disadvantage of this method is that when n and k are small, R will be small and hence difficult to measure accurately. It may be possible to use objectives of higher numerical aperture which would increase the angle of incidence, and thus increase the sensitivity and extend the range of this method.

D. Transmission

Another method of determining k is to do a direct transmission experiment. The feasibility of a transmittance measurement in regions of low reflectivity is demonstrated by the fact that reflection from the back surface of a crystal is occasionally observed, necessitating a correction to the observed reflectance.[11] It is extremely tedious to do this experiment properly. The measured transmittance must be corrected for reflection losses and for Beer's law deviations, etc. As a special project[16] attempts were made to measure both the reflectance and transmittance of several systems including liquid solutions, thin films, etc. A dual beam UV-visible recording spectrophotometer was used for the transmission measurements, and the reflection microspectrophotometer was used for reflection measurements. It was found that systems which showed any structure in the reflectance spectrum (i.e., an increase in reflectance from 4% to 8% as the band was traversed) were so opaque

that the transmission spectrum could not be measured over most of the spectrum (a broad band flat on top due to total absorption was obtained). Thus, apparently when k is small enough to allow transmittance to be measured, the associated reflectance is dominated by n. If R is dominated by n, then it is insensitive to the value of k, and thus the method will be insensitive. By the very nature of the experiment, it cannot be applied in regions of strong absorption, although these are usually the regions of interest. Therefore, this method is not very attractive.

E. Reflectance in a Different Medium

1. Introduction

Vincent-Geisse et al.[21,28] working in the IR region reported a method of determining optical constants from normal incidence reflectance measurements made on crystals coated with thin films.

The original technique[28] required several measurements to be made as the crystal was successively coated (by vapor deposition) with several layers of a thin film (approximately 1/4 wavelength) of a transparent solid of known thickness and refractive index. A graphical procedure was then used to obtain the optical constants (n and k) of the crystal. In a later modification,[21] the procedure was simplified somewhat by making three reflectance measurements successively on the bare crystal,

the crystal overlaid with a thin film (1/4 wavelength) of solid, and the crystal overlaid with two thicknesses of solid. The thickness of the film had to be determined independently. Their procedure appears to have attracted little attention, probably because of the experimental difficulty of applying and measuring the thickness of the solid layers and the fact that three reflectance measurements are required at each frequency. Apparently, they made no attempt to use liquids as the mediums of different refractive index; indeed, it would likely be experimentally difficult to produce thin stable layers of liquid of the correct thickness without using solid windows (which would in turn complicate the procedure). Schatz, Maeda, et al.[23,24] working in the IR region have considered the interpretation of reflectance measurements made from surfaces covered by a transparent window of known refractive index. However, they do not derive the optical constants by comparing reflectances in two different mediums; rather, they modify the usual Kramers-Kronig analysis to correct for the change in reflectance due to the presence of the window. Therefore, their work is actually a normal incidence Kramers-Kronig method (section IV. B) and bears only an indirect relation to the methods considered in this section.

In this laboratory we have developed a new method of determining optical constants from normal incidence reflectance measurements made in two mediums of different refractive index (one medium may be air). Our method represents an application of the principle of reflectance in different mediums which is somewhat different from that used by Vincent-Geisse et al. The Vincent-Geisse method[21,28] uses very thin (1/4 wavelength) films of the medium of different refractive index; their equations contain terms for the film thickness, phase difference for light traversing the film, etc. In our method the different medium is thick, occupying all the space between the crystal surface and the microscope objective (approximately 1 mm). The resulting equations are simpler and contain fewer terms than those in the Vincent-Geisse method. In fact our equations are not equivalent to the Vincent-Geisse equations (which cannot be used with our data). We have derived the theoretical equations for this reflectance in a different medium method and these are presented in section IV. E. 2; the errors associated with this method are discussed in section IV. E. 3; and experimental data demonstrating this method are presented in section IV. E. 4.

2. Theory

At normal incidence the real index of refraction is equal to the real part of the complex index of refraction;[1] only the normal incidence case will be considered. For light normally incident from medium one with refractive index n_1 onto medium two with refractive index n_2, the amplitude of the reflected wave is

$$r_{12} = \frac{n_2-n_1}{n_2+n_1}. \qquad \text{eq. 4-26}$$

If medium two is absorbing, then $\tilde{n}_2 = n_2-ik_2$, and the amplitude of the reflected wave is given by[17]

$$\tilde{r}_{12} = \frac{n_2-ik_2-n_1}{n_2-ik_2+n_1}. \qquad \text{eq. 4-27}$$

The intensity of the reflected wave is[17]

$$R_{12} = \tilde{r}_{12}\cdot\tilde{r}_{12}^{*} = r_{12}^{2} = \frac{(n_2-n_1)^2+k_2^2}{(n_2+n_1)^2+k_2^2}. \qquad \text{eq. 4-28}$$

This equation may be applied to the case where light is normally incident from a non-absorbing medium of refractive index n_1 onto an absorbing crystal with optical constants

n_2 and k_2. If the refractive index of the medium (n_1) is known and if R_{12} is measured, then eq. 4-28 has only n_2 and k_2 as unknowns. For the case when medium one is air, then n_1 is essentially 1.0 and the reflectance is

$$R = \frac{(n_2-1)^2+k_2^2}{(n_2+1)^2+k_2^2} , \qquad \text{eq. 4-29}$$

(which is the same as eq. 4-3). This equation also has only n_2 and k_2 as unknowns. Therefore, the two equations 4-28 and 4-29 can be solved simultaneously for the two unknowns n_2 and k_2. Substituting n_ℓ for n_1 and R_ℓ for R_{12} when medium one is a liquid, and R_χ for R when medium one is air, the result for n_2 is

$$n_2 = \frac{n_\ell^2-1}{2}\left[\frac{n_\ell(R_\ell+1)}{(1-R_\ell)} - \frac{R_\chi+1}{1-R_\chi}\right]^{-1} . \qquad \text{eq. 4-30}$$

The Fresnel equation (eq. 4-29) may then be solved for k_2 which gives

$$k_2 = \left[\frac{R_\chi(n_2+1)^2 - (n_2-1)^2}{1-R_\chi}\right]^{1/2} . \qquad \text{eq. 4-31}$$

Therefore, if the reflectance from a crystal is measured at a given frequency both in air and in a liquid of known refractive index, then n and k of the crystal at that frequency may be calculated from eq. 4-30 and 4-31, respectively. θ at that frequency may then be calculated from eq. 4-4 or 4-5; from eq. 4-4,

$$\cos\theta = \frac{1}{2\sqrt{R}}\left[\frac{R-1}{n_2} + 1 + r\right] \qquad \text{eq. 4-32}$$

and

$$\theta = \arccos\left[\frac{1}{2\sqrt{R}}\left(\frac{R-1}{n_2} + 1 + R\right)\right]. \qquad \text{eq. 4-33}$$

Equations 4-30 and 4-31 are valid for any non-absorbing medium; the second medium may be a solid or gas as well as a liquid. Also, it is not necessary to assume that the absorption bands are isolated; overlapping bands can be analyzed by this technique.

If it is desired to use two mediums, neither of which is air, then eq. 4-28 may be rewritten as

$$R_{13} = \frac{(n_2-n_3)^2 + k_2^2}{(n_2+n_3)^2 + k_2^2}, \qquad \text{eq. 4-34}$$

where R_{13} is the measured reflectance from the system when covered with a transparent medium of known refractive index, n_3; as in eq. 4-28, n_2 and k_2 are the unknown optical constants of the system being studied. When eq. 4-28 and 4-34 are solved simultaneously for n_2 and k_2 the results are:

$$n_2 = \frac{n_1^2-n_3^2}{2}\left[\frac{n_1(R_{12}+1)}{1-R_{12}} - \frac{n_3(R_{13}+1)}{1-R_{13}}\right]^{-1}; \qquad \text{eq. 4-35}$$

and

$$k_2 = \left[\frac{R_{12}(n_2+n_1)^2 - (n_2-n_1)^2}{1-R_{12}}\right]^{1/2}. \qquad \text{eq. 4-36}$$

Eq. 4-35 and 4-36 could, for example, be applied to the case of strongly absorbing liquids covered by a solid transparent window[23,24,29] by making reflectance measurements through two different windows of known refractive index n_1 and n_3 (corrections for reflectance from the first surface of the window, etc.[29] would have to be made). The method could also be extended to include absorbing mediums by substituting $\tilde{n}_1 = n_1 - ik_1$ in eq. 4-27 and proceeding with the derivation as before. If both n_1 and k_1 are known, no new unknowns appear in the resulting equations. However, the correction term discussed in section III. E would have to be modified by substituting $\tilde{n}_2 = n_2 - ik_2$ in the Fresnel equation. In addition to being more complicated to use, an absorbing medium would also reduce the light intensity reaching the detector. Thus, it is preferable to avoid absorbimg mediums.

One disadvantage of this method is the requirement of knowing the refractive index of the liquid at each wavelength of interest (in general, refractive index is a function of frequency and temperature). This information is often not readily available. A useful approximation is to assume that refractive index is constant in regions of the spectrum void of nearby absorption bands.

3. Potential Errors

Since the bracketed term in eq. 4-30 involves the difference of two experimentally determined numbers, under certain conditions random errors in the reflectance measurements may cause extremely large errors in the calculated value of n_2. The total differential is inappropriate in this case, but the magnitude of the error can be assessed as follows.

Let $A \equiv \frac{n_\ell (R_\ell + 1)}{1 - R_\ell}$ and $B \equiv \frac{R_\chi + 1}{1 - R_\chi}$.

Then eq. 4-30 may be rewritten as

$$n_2 = \frac{n_\ell^2 - 1}{2} \left[A - B \right]^{-1} . \qquad \text{eq. 4-37}$$

ΔA, the change in A, produced by ΔR_ℓ, the change in R_ℓ, is

$$\Delta A = \frac{2 n_\ell \Delta R_\ell}{(1 - R_\ell)^2} , \qquad \text{eq. 4-38}$$

neglecting higher order terms.

Similarly,

$$\Delta B = \frac{2 \Delta R_\chi}{(1 - R_\chi)^2} . \qquad \text{eq. 4-39}$$

Then,

$$n_2 \pm \Delta n_2 = \frac{n_\ell^2 - 1}{2} \left[(A \pm \Delta A) - (B \pm \Delta B) \right]^{-1},$$

or in order to assess the maximum effect of the errors,

$$n_2 \pm \Delta n_2 = \frac{n_\ell^2 - 1}{2} \left[\frac{1}{A - B \pm (\Delta A + \Delta B)} \right]^{-1}. \qquad \text{eq. 4-40}$$

Δn_2, the change in n_2 due to a change in R and R_χ, is found by subtracting eq. 4-37 from 4-40

$$\Delta n_2 = \frac{n_\ell^2 - 1}{2} \left[\frac{1}{A - B \pm (\Delta A + \Delta B)} \right]^{-1} - \frac{n_\ell^2 - 1}{2} \left[\frac{1}{A - B} \right]^{-1} =$$

eq. 4-41

$$\frac{n_\ell^2 - 1}{2} \left[\frac{\pm (\Delta A + \Delta B)}{(A - B)\left[A - B \pm (\Delta A + \Delta B) \right]} \right]^{-1}.$$

From eq. 4-37

$$A - B = \frac{n_\ell^2 - 1}{2 n_2}.$$

Substituting in eq. 4-41

$$\Delta n_2 = \pm \frac{n_2 (\Delta A + \Delta B)}{A - B \pm (\Delta A + \Delta B)},$$

or substituting again,

$$\Delta n_2 = \pm \frac{n_2 (\Delta A + \Delta B)}{\frac{n_\ell^2 - 1}{2 n_2} \pm (\Delta A + \Delta B)}. \qquad \text{eq. 4-42}$$

The relative error in n_2 is

$$\frac{\Delta n_2}{n_2} = \frac{\pm(\Delta A+\Delta B)}{\frac{n_\ell^2-1}{2n_2} \pm (\Delta A+\Delta B)} \cdot \qquad \text{eq. 4-43}$$

From eq. 4-42 it can be seen that as $(\Delta A+\Delta B)$ approaches the value of $\frac{n_\ell^2-1}{2n_2}$, the error in n_2 may approach infinity; from eq. 4-40 if $(\Delta A+\Delta B)$ exceeds $\frac{n_\ell^2-1}{2n_2}$, the calculated value of $n_2 \pm \Delta n_2$ may become negative.

From eq. 4-43 it can be seen that the relative error in n_2 is decreased by increasing the value of n_ℓ (using a liquid with a larger refractive index); it can also be seen that the relative error increases with increasing values of n_2 (assuming no change in $\Delta A+\Delta B$).

In section III F 2 it was shown that $\Delta R \approx \pm .02R$. When this is substituted in eq. 4-38 and 4-39

$$\Delta A = \frac{.04 n_\ell R_\ell}{(1-R_\ell)^2} \qquad \text{eq. 4-44}$$

and

$$\Delta B = \frac{.04 R_\chi}{(1-R_\chi)^2} \cdot \qquad \text{eq. 4-45}$$

Thus, ΔA and ΔB, and hence Δn_2, increase with increasing R. Equations 4-43, 4-44, and 4-45 can be combined to assess the maximum relative error in the value of n_2, assuming

R_ℓ and R_χ are known. If R_χ and R_ℓ are about .8, then $(\Delta A+\Delta B)$ is about 2. If $n_\ell = 1.4$, eq. 4-43 implies that calculated values of $n_2 > .2$ will be unreliable. If R_χ and R_ℓ are about .2, then $(\Delta A+\Delta B)$ is about .03. From eq. 4-43, the error in n_2 when $n_2 \approx 4$ is $\approx \pm 30\%$; when $n_2=3$, the error is $\approx \pm 20\%$.

Since A and B are similar in form, a systematic error which affects R measurements in both liquid and air will produce errors in the values of A and B which are similar in magnitude and have the same sign. Substituting in eq. 4-37 and assuming a positive error,

$$n_2 + \Delta n_2 = \frac{n_\ell^2-1}{2} [(A+\Delta A)-(B+\Delta B)]^{-1}$$

or

$$n_2 + \Delta n_2 = \frac{n_\ell^2-1}{2} [A-B+(\Delta A-\Delta B)]^{-1}.$$

Thus, if $\Delta A \approx \Delta B$ there is very little error in n_2. Therefore, systematic errors such as imperfections in the crystal surface, misalignment, etc. cause much less error in n_2 than do random errors of the same size.

Eq. 4-31 may be rewritten as

$$k_2 = \left[\frac{4n_2}{1-R_\chi} - (n_2+1)^2\right]^{1/2}.$$

Although n_2 is insensitive to systematic errors, from this equation it can be seen that an error in the crystal reflectance produces an error in k_2 which increases with in-

creasing R_x regardless of whether it is systematic or random. Thus, in order to get accurate values of k, it is necessary to use high quality crystals.

4. Experimental Verification

In order to compare the reflectance in a different medium method with the Kramers-Kronig method, the reflectance spectrum of face 3 of BDP was measured in benzene (refractive index 1.5011)[20] and iso-octane (refractive index 1.3915)[20] using the technique described in section III. E. The spectra are reported in figures 3-2 and 3-3. The reflectance values were used to calculate n, ε, and θ from eq. 4-30, 4-31, 4-2, and 4-33 assuming the refractive index of the liquids to be constant. Figure 4-6 shows the results for n at long wavelengths. The solid line is the literature value[11] which was calculated by the Kramers-Kronig analysis. The dashed lines indicate the maximum and minimum values which would be produced by an error of ±1% in the reflectance measurements. The calculated values of n from both liquids agree with the Kramers-Kronig values within the expected limits of error (in section III. F. 2 the maximum error in the reflectance measurements was shown to be ±2% R). Calculated values of ε and θ in this region are not in good agreement with the literature values.[11] This is because R is dominated by n in this region since n is large and k is small; thus

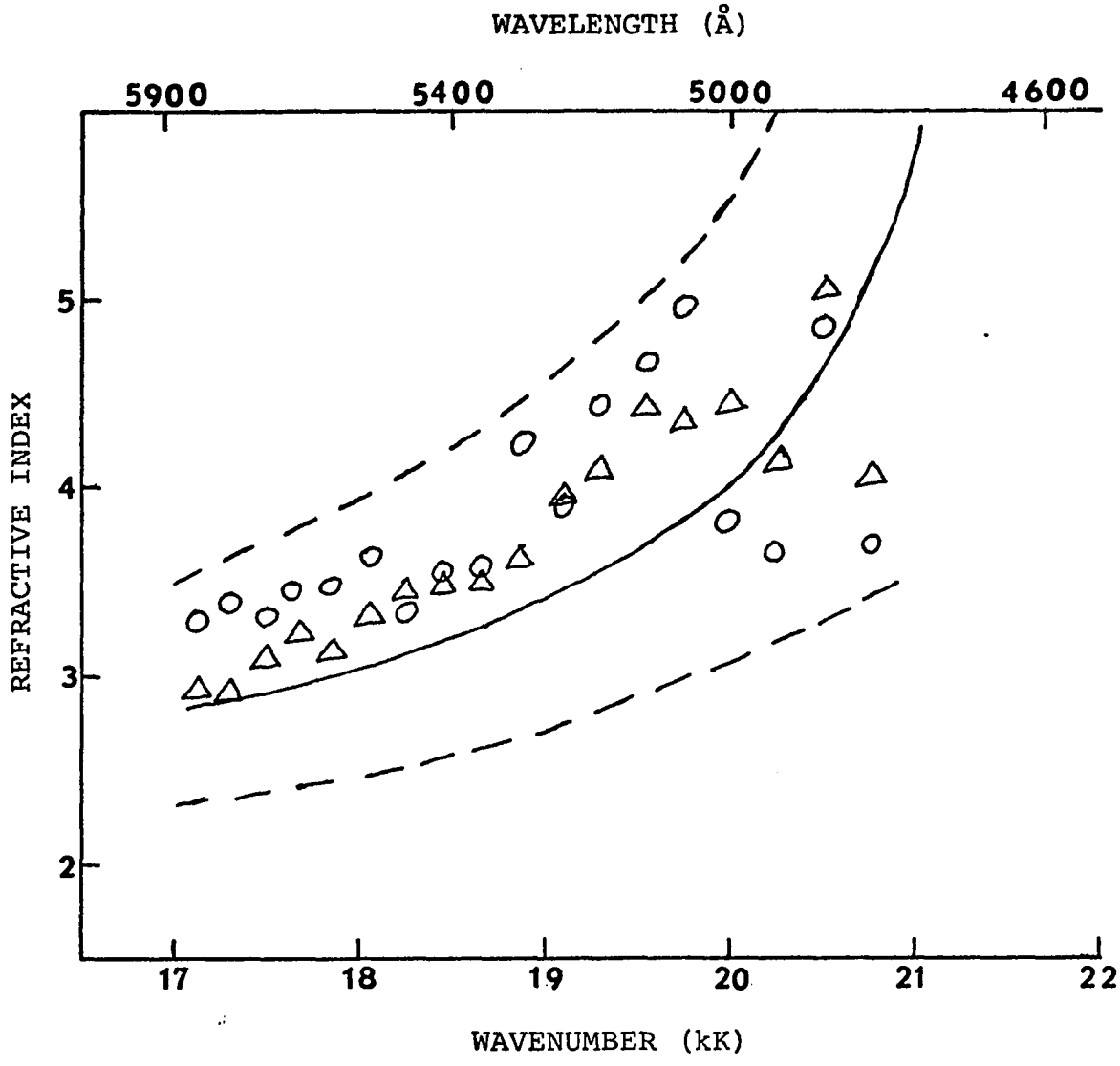

Figure 4-6. Comparison of refractive index values at long wavelengths of face 3 of BDP determined by Kramers-Kronig analysis[11] (solid line) and by reflectance in a different medium method (iso-octane data = 0, benzene data = Δ). Dashed lines indicate error range for ±1% error in R.

R is insensitive to the value of k. This causes large errors in the calculated values of ε and θ. In the region of the spectrum from about 20.5 to 25.0 kK (the middle of the absorption band), n, ε and θ are all extremely error prone (see error discussion in previous section).

Figure 4-7 shows the results for n at short wavelengths. As in figure 4-6, the solid line is the literature Kramers-Kronig value,[11] and the dashed lines represent the error limits for a ±1% error in R. The values from the iso-octane data agree with the Kramers-Kronig values within experimental error. The values from the benzene data are not in agreement. Benzene begins to absorb light in this spectral region and its refractive index is probably changing with frequency. The data were not corrected for these effects.

Figure 4-8 shows the results for ε at short wavelengths. The solid line is again from a Kramers-Kronig analysis,[11] and the dashed lines again represent the error range corresponding to an error of ±1% R. Only the iso-octane data are shown since the results for n have already shown the benzene data to be useless at these short wavelengths. The values of ε calculated from the iso-octane data agree with the Kramers-Kronig values within experimental error. Figure 4-9 shows that the results for θ at short wavelengths (calculated from the iso-octane data) determined by the reflectance in a different medium method also agree

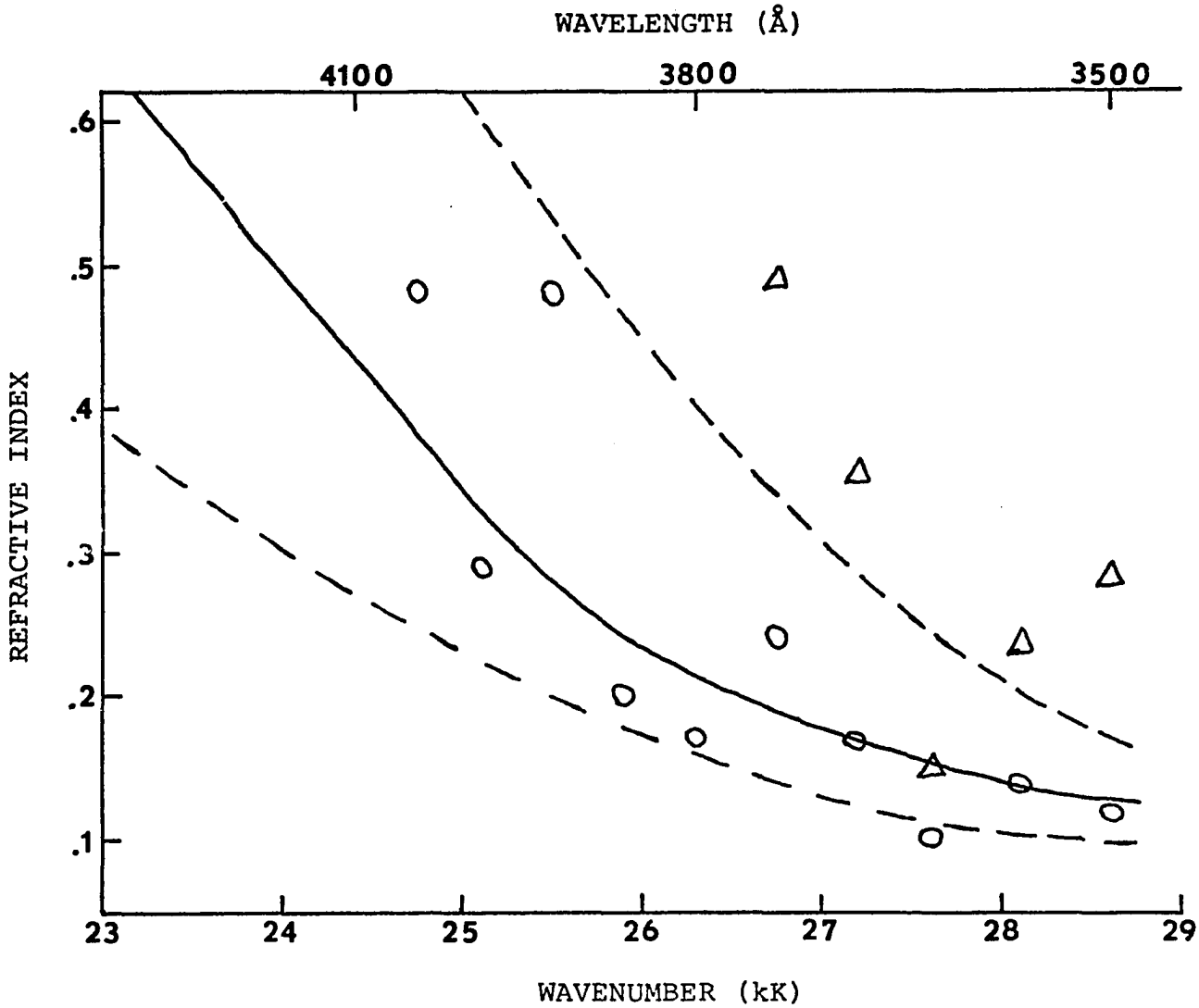

Figure 4-7. Comparison of refractive index values at short wavelengths of face 3 of BDP determined by Kramers-Kronig analysis[11] (solid line) and by reflectance in a different medium method (iso-octane data = 0, benzene data = Δ). Dashed lines indicate error range for ±1% error in R.

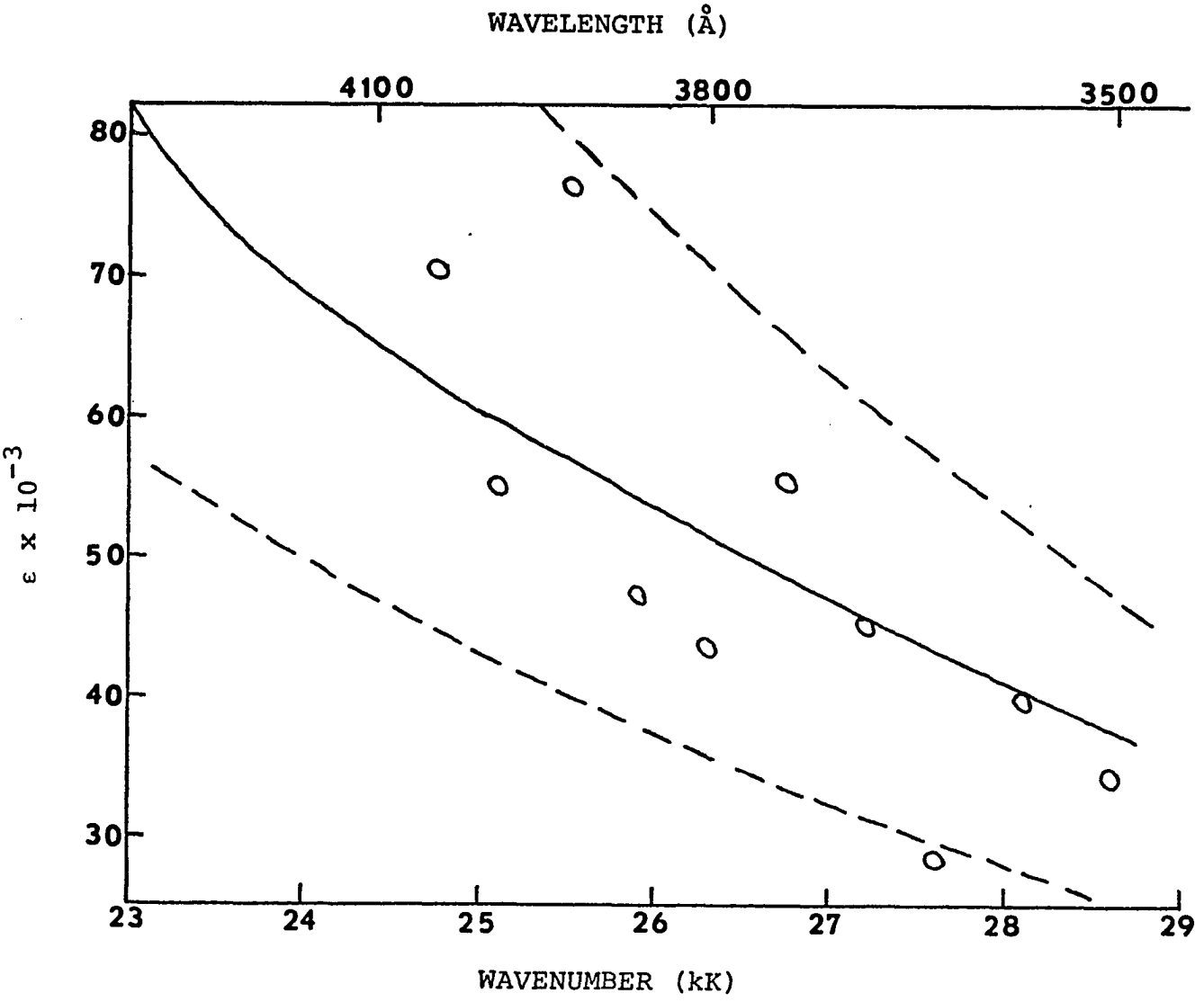

Figure 4-8. Comparison of molar extinction coefficient values for face 3 of BDP determined by Kramers-Kronig analysis[11] (solid line) and by reflectance in a different medium method (iso-octane data = 0). Dashed lines indicate error range for ±1% error in R.

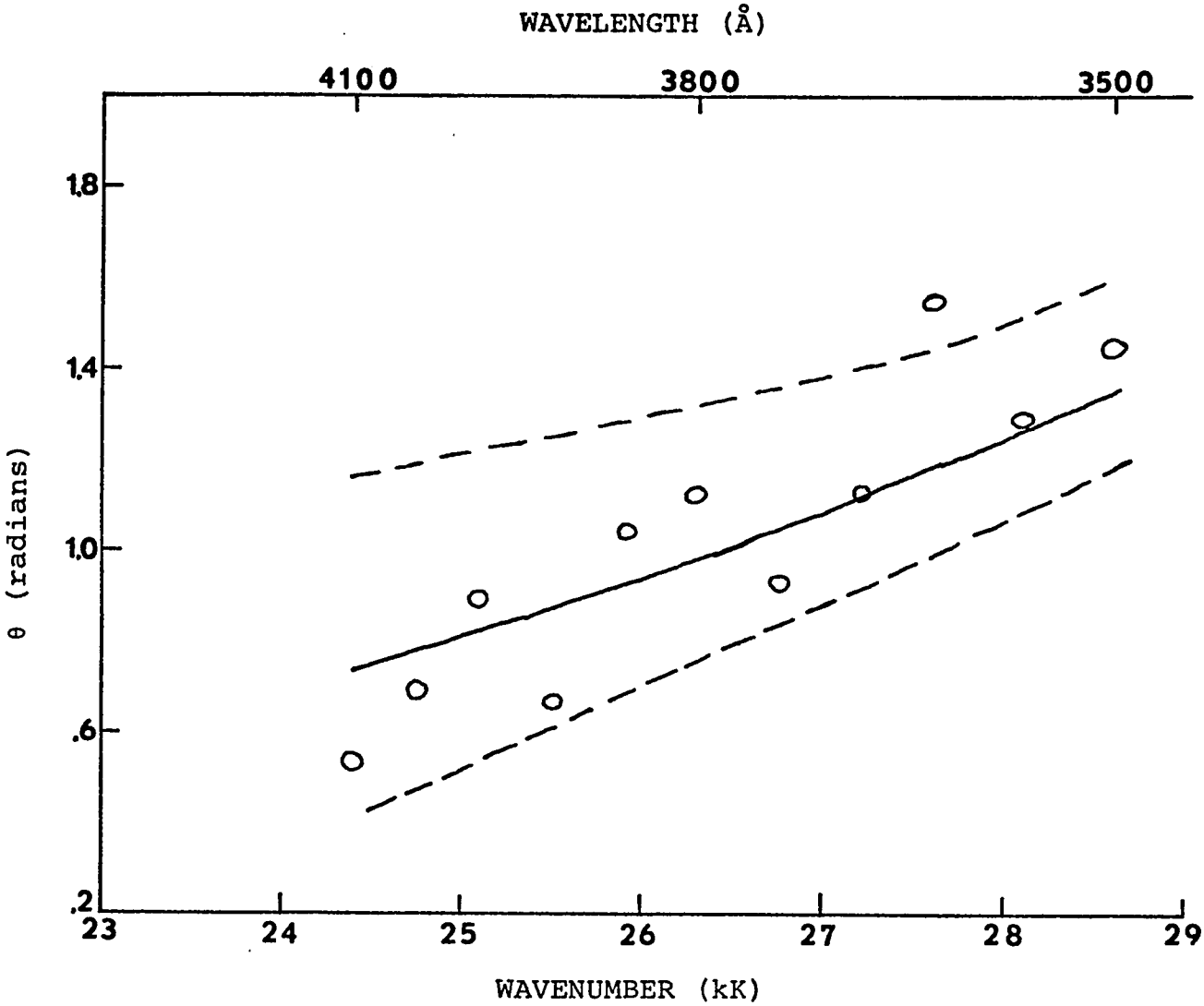

Figure 4-9. Comparison of phase angle values of face 3 of BDP determined by Kramers-Kronig analysis[11] (solid line) and by reflectance in a different medium method (iso-octane data = 0). Dashed lines indicate error range for ±1% error in R.

with the Kramers-Kronig values within experimental error. This is especially significant since it is only necessary to know the value of θ at a few frequencies in order to uniquely determine the adjustable parameters in the Kramers-Kronig analysis. The most favorable region of the spectrum for determining θ (and ε) is in a region of the reflectance band where n is small and k is relatively large.

In order to further demonstrate the self consistency of the liquid medium method, a set of reflectance measurements was taken on face 3 of BDP using four different liquids and air. The liquids used were the following: freon (1,1,2 trichlorotrifluoroethane), refractive index 1.3557; iso-octane, refractive index 1.3915; carbon tetrachloride, refractive index 1.4601; and benzene, refractive index 1.5011.[20] The observed spectra are shown in figures 4-10 and 4-11. Unfortunately, the crystal used was not high quality, as evidenced by the reduced intensity of the air spectrum (compare figure 4-10 to figure 4-1). Since the calculated values of n are less sensitive than k to systematic errors such as crystal surface defects (probably the cause of poor quality of the crystal used for this data set), only the values of n are reported. Figure 4-12 shows the results at long wavelengths. The solid line is the average value calculated from the four liquids; the dashed lines are the approximate error range for an error of ±1% R. Figure 4-13 shows the results for

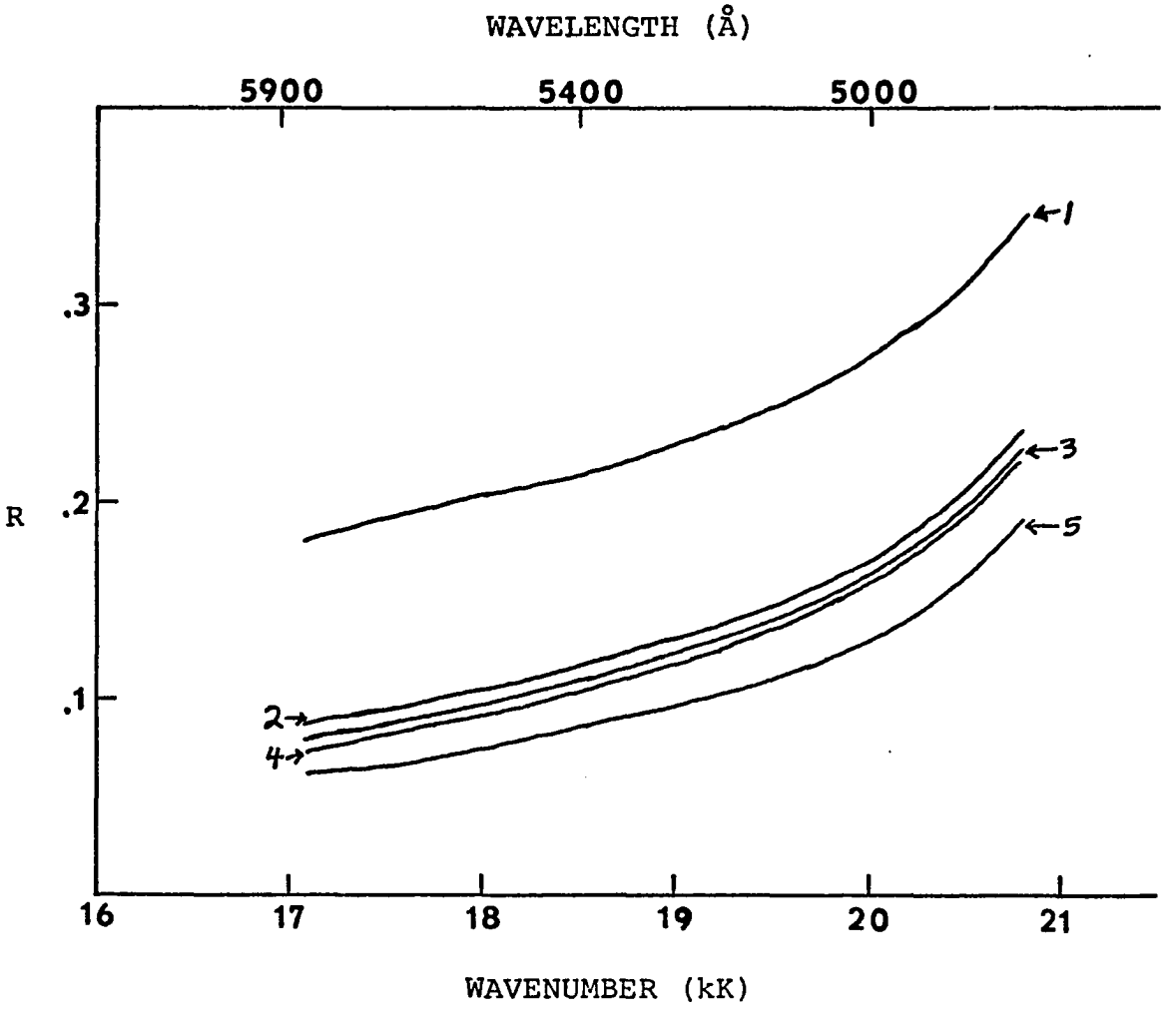

Figure 4-10. Reflectance Data from BDP at Long Wavelengths for Self-consistency Comparison. Curves 1, 2, 3, 4, and 5 Represent the Reflectance in Air, Freon, Iso-octane, Carbon Tetrachloride, and Benzene Respectively.

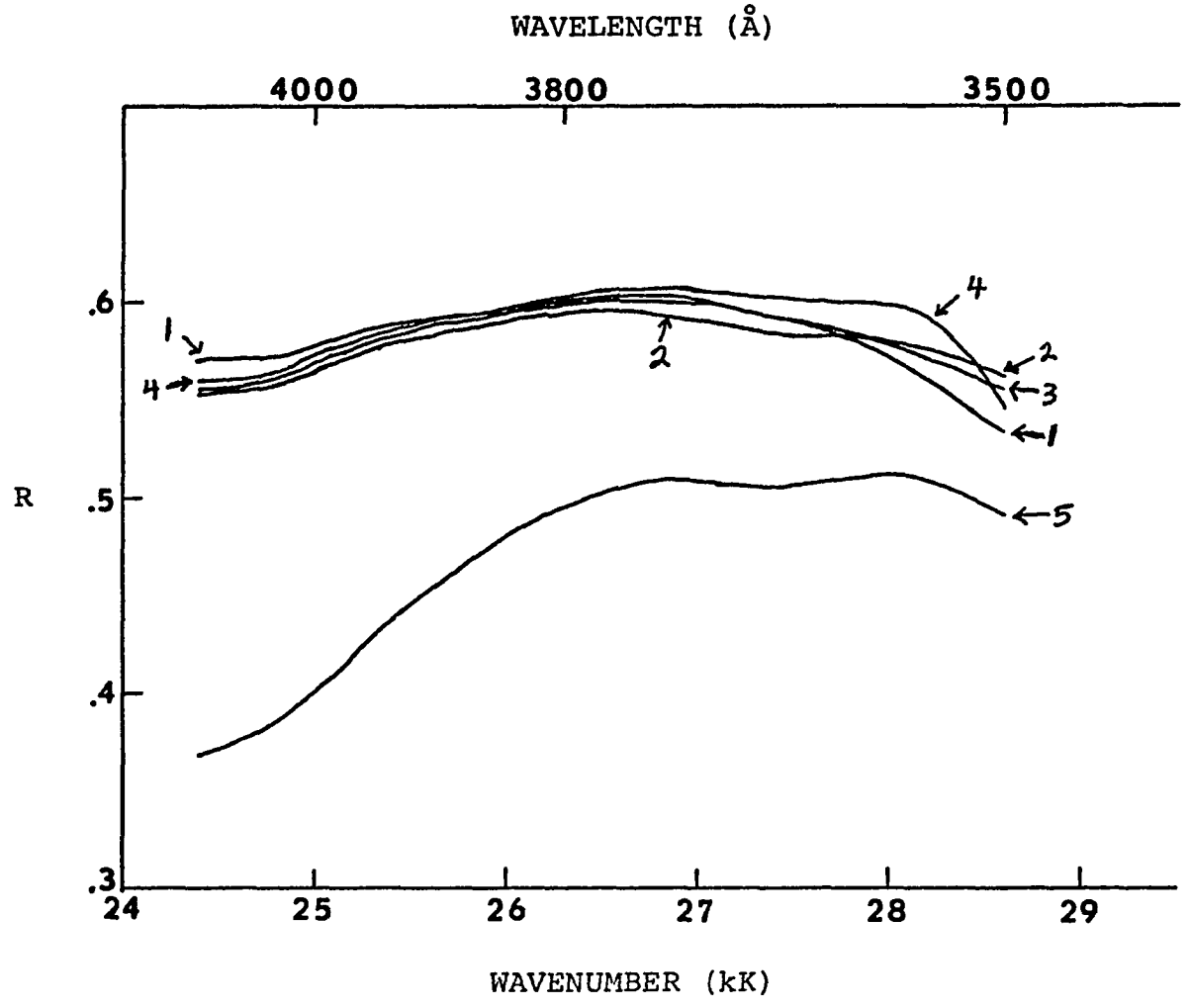

Figure 4-11. Reflectance Data from BDP at Short Wavelengths for Self-consistency Comparison. Curves 1, 2, 3, 4, and 5 Represent the Reflectance in Air, Freon, Iso-octane, Carbon Tetrachloride, and Benzene Respectively.

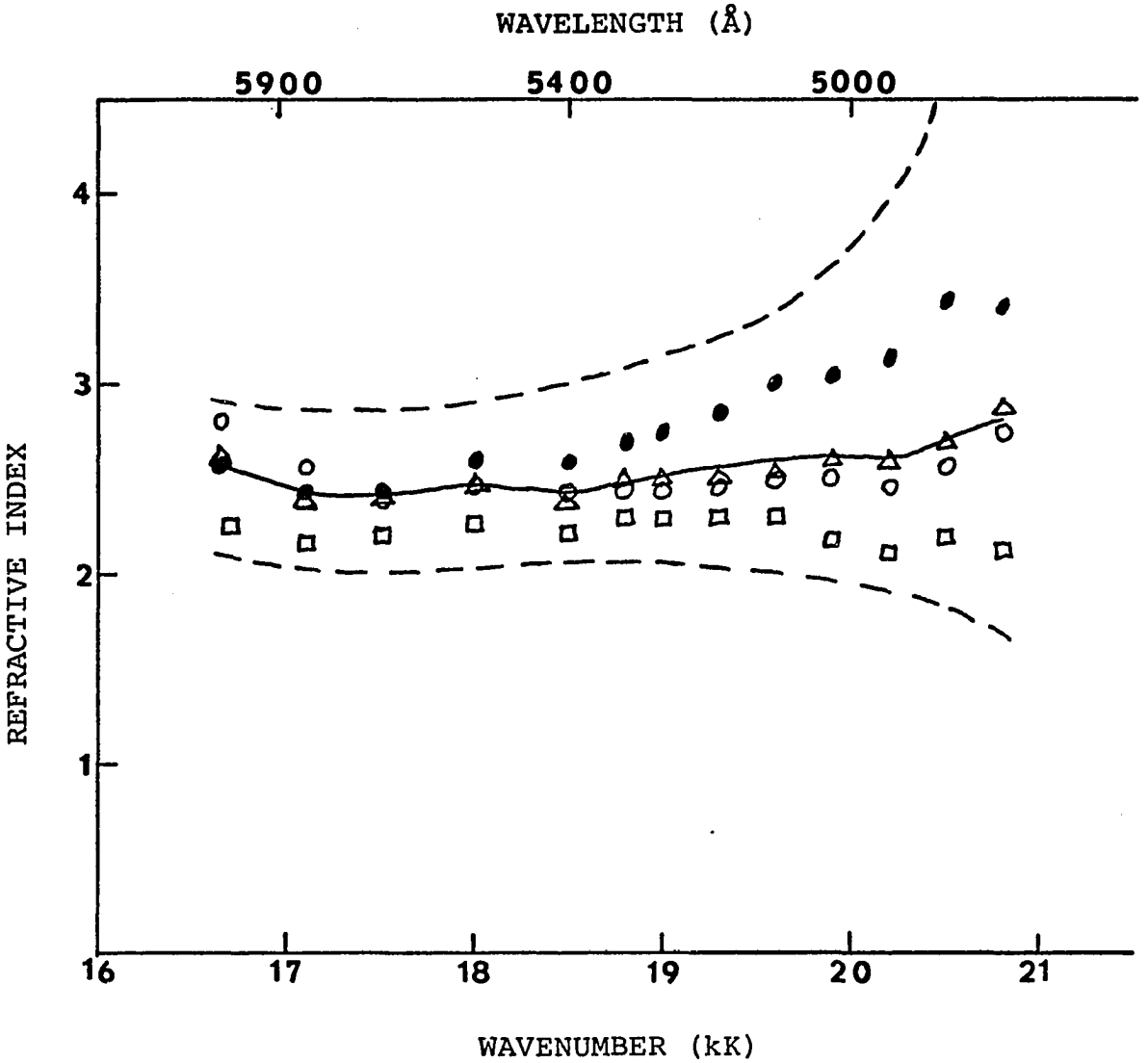

Figure 4-12. Self consistent values of refractive index at long wavelengths for different liquids using reflectance in a different medium method. Iso-octane data = 0, freon data = Δ, benzene data = ●, carbon tetrachloride data = □. Solid line is average value; dashed lines indicate error range for ±1% error in R.

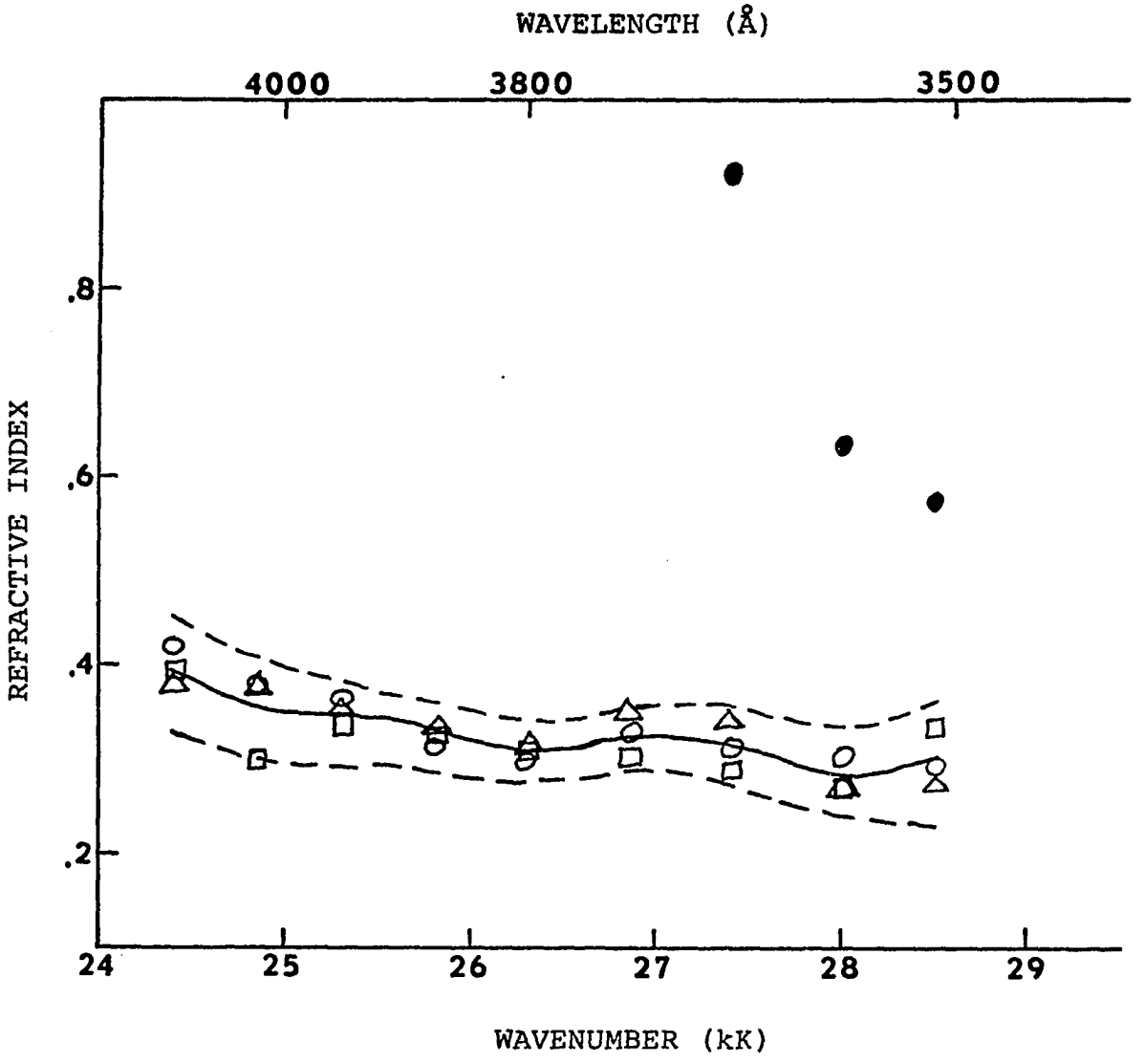

Figure 4-13. Self consistent values of refractive index at short wavelengths for different liquids using reflectance in a different medium method. Iso-octane data = 0, freon data = Δ, benzene data = ●, carbon tetrachloride data = □ . Solid line is average of iso-octane, freon, and carbon tetrachloride data; dashed lines indicate error range for ±1% error in R.

short wavelengths. The solid line is the average value calculated from the freon, iso-octane, and carbon tetrachloride data; the dashed lines are the approximate error band from an error of ±1% R. In the long wavelength region all four liquids are in agreement with each other within experimental error. In the short wavelength region, the benzene data set is the only one not in agreement. As stated above this is probably due to the absorption of light by benzene at these wavelengths, and an accompanying change in its refractive index, for which no correction has been made. Since k is calculated from the refractive index of the crystal and the crystal reflectance in air, the self consistency in the values of n also implies self consistency in the values of k and hence ε and θ.

The "reflectance in a different medium" technique can in principle be used to determine optical constants over all the observable spectrum without the necessity of the Kramers-Kronig calculation. However, the measurements become extremely tedious near the peak of the absorption band. Therefore, the technique's greatest utility will likely be as a method of determining the constants in the Kramers-Kronig calculation. The data taken for the reflectance in a different medium method can be used directly in the Kramers-Kronig analysis; no additional measurements are required. Note that in the preceeding application usable data is obtained about half way up the absorption

band or almost on top of the reflectance band. Thus, θ values could be determined from reflectance measurements made near the absorption peak in regions where R is large (see Fig. 4-1 and 4-9). This has the following advantages over the k=0 method of determining the adjustable parameters; the phase assignments are made nearer the region of interest; R is larger than in the k=0 region and therefore easier to determine accurately. Taken together the reflectance in a different medium method combined with the application of the extended mean value theorem (section IV. B. 2) provide a simple generally applicable method of obtaining reliable optical constants.

APPENDIX A

REFLECTANCE SPECTRA OF TWO PROMINENT FACES OF $BDP^{+}Cl^{-}$ (R max 4560 Å).

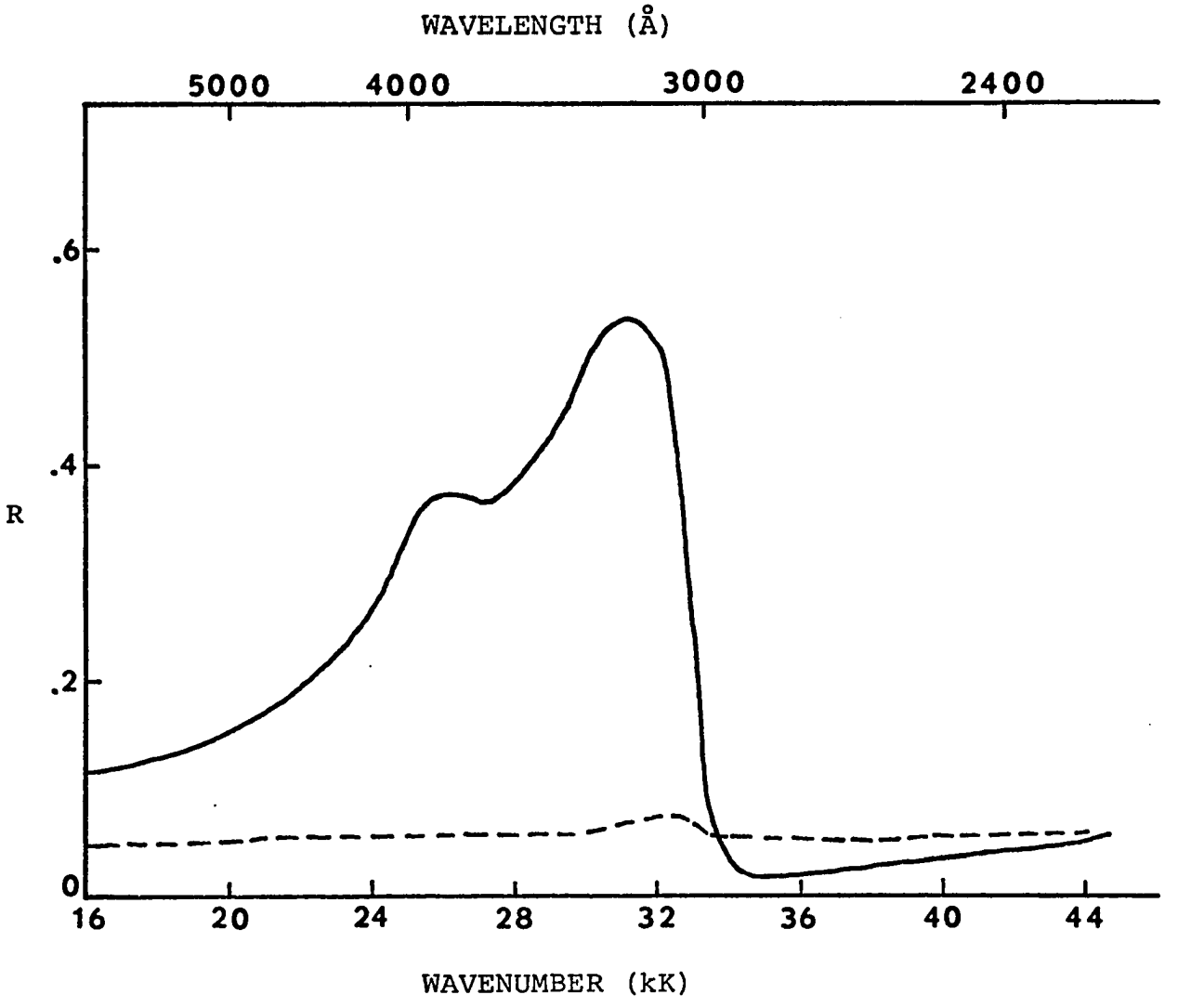

Figure A-1. Polarized reflection spectrum for a commonly observed prominent face of $BDP^{+}Cl^{-}$. Solid line is Rmax (4560 Å); dashed line is Rmin.

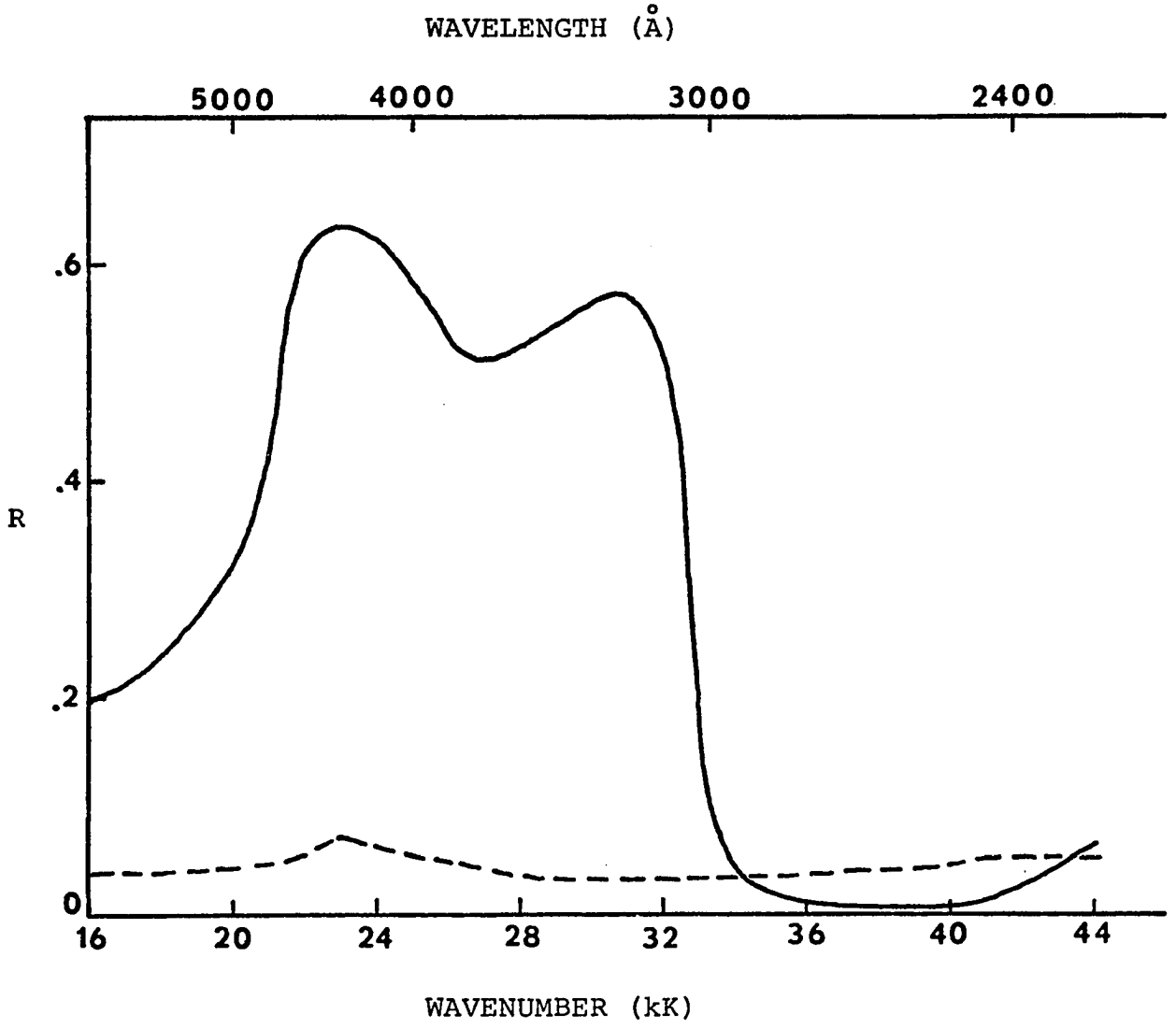

Figure A-2. Polarized reflection spectrum of another face of $BDP^{+}Cl^{-}$. Solid line is Rmax (4560 Å); dashed line is Rmin.

APPENDIX B

Computer Program for Kramers-Kronig Calculation

This program is based on the extended mean value theorem method of calculating the phase angle, but can also be used with the constant R method. The equations used are 4-9, 4-20, and 4-21. The program is designed to use raw reflection intensity values (single beam mode) taken directly from the recorder paper (read from 0 to 100 full scale) along with the attenuation settings. The program calculates the reflectance at each wavelength, and converts the wavelengths to units of circular frequency. Then it generates reflectance values as a function of frequency in .1 kK increments by interpolating from the entered data points (assuming that reflectance is a linear function of frequency between adjacent entered data points). Thus, it is not necessary to enter the data in constant frequency or wavelength increments, and the data points may be widely spaced in regions of the spectrum where the reflectance is a linear function of frequency. The original data is not used in the subsequent calculations and is not printed out. The integration over circular frequency is performed

using the trapezoid rule.

An option to define θ at two wavelengths in the observed region is included. If this option is not exercised, then the phase is calculated using the constant R method rather than the extended mean value theorem method.

The known reflectance spectrum of the reference mirror is incorporated into the data set via the mirror factor deck. The program takes as a value for the mirror factor at any wavelength, the value listed in the mirror factor deck at the nearest adjacent wavelength. Thus, the mirror factor deck need not list values for each frequency or even be listed in constant frequency or wavelength increments. Although the program is designed to use raw intensity measurements, it can easily be used with conventional reflectance spectra by substituting a unity mirror factor deck in place of the usual deck. A unity deck is conveniently made with only two data cards having a mirror factor of 1.0 (one card for a low frequency and one for a high frequency, both frequencies arbitrarily chosen beyond the spectral range of the instrument).

Equation 4-9 contains a singular point at $\omega = \omega_i$. An approach commonly used is to simply calculate the term in the integration corresponding to $\omega = \omega_i$ by taking a larger interval such that ω is less than ω_i at one end of the interval and ω is greater than ω_i at the other end. Since the resonance denominator approaches zero in

this region, it is not obvious that such a technique does not introduce error. An original approach is used in this program. The numerator of eq. 4-9 may be written $\ell n\frac{R(\omega)}{R(\omega_i)}$. Since reflectance values are always generated in .1 kK increments, $\frac{R(\omega)}{R(\omega_i)} \approx 1$ for points nearest the singular point. If $2 > x > 0$, then $\ln x = (x-1) - 1/2(x-1)^2 + 1/3(x-1)^3 \ldots .^{20}$ When $x \approx 1$, the first three terms of this series approximates $\ln x$ accurately to three significant figures (which is within the limits of experimental error in reflectance values). Since the total interval necessary to span the singular point is .2 kK, $R(\omega)$ is approximated as a linear function of ω. With these approximations eq. 4-9 is reduced to integrals of the form $C \int \frac{\omega^n}{\omega^2-\omega_i^2} d\omega$, where n = 2,3,1, or 0. These integrals can be evaluated explicitly. Values of θ calculated using this approximation for the singular point agreed with θ values calculated by the usual larger interval technique to better than three significant figures (i.e., within experimental error). Therefore, the larger interval technique introduces no error.

In the program output, the following information is printed at the top of a data table: MOL CON is the molar concentration of the crystal; DATA PTS is the number of data points entered; WLA and THETA at the left edge of the output are the lower energy wavelength and corresponding defined value of the phase angle; WLB and THETA at the right side of the heading are the higher

energy wavelength and defined value of the phase angle; RL and RW are the values of the constants in the mean value theorem for the low and high energy wings respectively; LWING and HWING are the values of the wings at the defining wavelengths. The rest of the data is printed in a table under the following headings: EXTC (10-3) is the molar extinction coefficient (ε) multiplied by 10^{-3} in units of (liters/mole)/cm; LOGWNO is the $\log_{10}$ of the wave number (cm^{-1}); CIRFREQ is the circular frequency in units of 10^{15} radians/sec; PHASE is the phase angle in radians; N is the real part of the index of refraction; K is the imaginary part of the index of refraction; WAVEL(A) is the wavelength in angstroms; WAVEN(KK) is the wave number in kilokaysers (i.e., 10^3 cm^{-1}); REFLECT is the reflectance. Following the data table, the absorption and reflection spectra are plotted on an arbitrary intensity scale selected such that the maximum value of both spectra fall at the top of the graph. The symbol for reflectance is *. The symbol for the extinction coefficient is + unless the value is negative in which case the absolute value is plotted using the symbol □ . At points where the spectra cross, the symbol X is used.

The specific program input consists of a mirror deck followed by a data deck. The mirror deck input is as follows. Card 1, column 1 to 3, number of wavelengths listed in mirror deck, format I3. Card 2 lists the plot

symbols: column 1 is blank; column 2 is + (extinction coefficient); column 3 is . (side border); column 4 is X (crossing of curves indicator); column 5 is I (top and bottom border); column 6 is □ (negative extinction coefficient); column 7 is * (reflection). Cards 3 to end of mirror deck contain the reflectance of the standard mirror at given wavelengths; columns 1 to 4, variable name V(I), format F4.0 is the wavelength in angstroms (deck must be ordered in increasing wavelength); columns 6 to 12, variable name F(I), format F10.5 is the reflectance of the standard mirror.

The mirror deck is followed immediately by the data deck whose input is as follows. Card 1, columns 1 to 10, variable name C, format F10.5, enter the molar concentration of the crystal (enter 1.0 if unknown); columns 11 to 14, variable name WLA, format F4.0, enter the shorter wavelength (angstroms) at which a value of θ will be defined; columns 15 to 30, variable name THA, format F16.8, enter the value of θ (radians) at the shorter defining wavelength; columns 31 to 34, variable name WLB, format F4.0, enter the longer wavelength (angstroms) at which θ will be defined; columns 35 to 50, variable name THB, format F16.8, enter the value of θ (radians) at the longer defining wavelength; column 52, variable name MG, enter 1 for punched card output. Card 2 contains the title of the run, format 20A4 (leave first space blank). Cards 3 through N comprise the rest of the data and include the various intensity readings at each wavelength (this part of the deck must be ordered

in increasing wavelength). Card 3, columns 1 to 4, variable name XLAM, format F4.0, enter wavelength (angstroms); columns 5 to 14, variable name XTAL, format F10.5, enter raw intensity reading for the crystal (do not enter 0.0); columns 15 to 24, variable name XMIR, format F10.5, enter raw intensity reading for the standard mirror (do not enter 0.0); columns 25 to 34, variable name XBAC, format F10.5, enter the raw intensity reading for the stray light; columns 35 to 44, variable name ASX, format F10.5, enter the attenuation setting for the crystal readings; columns 45 to 54, variable name ASM, format F10.5, enter the attentuation setting for the mirror readings; columns 55 to 64, variable name ASB, format F10.5, enter the attenuation setting for the stray light readings. Cards 4 through N-1, enter the wavelength and intensity readings exactly as for card 3 (leave attenuation settings blank). If a different attenuation setting was used for part of the data, along with the other information reenter the attenuation settings on the card corresponding to the wavelength at which the change was made exactly as for card 3. Card N (the last card in the data deck) contains the same information as cards 4 through N-1 and in column 70, variable name JERK, format I6, enter 1 (indicate last card).

The program is listed on the following pages. The assistance of Carl C. Zinsser, Ph.D. in writing this program is gratefully acknowledged.

```
      DIMENSION R(350),F(240),V(240),W(350),Z(350),WL(350),WKK(350),
     2 E(350),TITLE(20) , LPOT(103)
      READ(5,5)II
    5 FORMAT(I3)
      READ(5, 602) LBB, LPL, LDT, LXX,LXI, LXB ,LST
  602 FORMAT(7A1)
      DO 3 I=1,II
    3 READ(5,2)V(I),F(I)
    2 FORMAT(F4.0,6F10.5,I6)
    4 READ(5,400) C, WLA, THA, WLB,THB, MG
  400 FORMAT(F10.5, 2(F4.0, F16.8), I3)
      IF(C) 328, 328, 246
  246 READ(5,7) TITLE
    7 FORMAT(20A4)
      DO 300 I=1, 350
      READ(5,2) XLAM, XTAL, XMIR, XBAC, ASX, ASM, ASB, JERK
      IF(ASX) 313,312, 313
  313 BSX=ASX
      BSM=ASM
      BSB=ASB
  312 R(I)=XTAL*BSX
      Z(I)=XLAM
      WKK(I)=XMIR*BSM
      W(I)=XBAC*ASB
      IF(JERK)310, 300, 310
  310 N=I
      GO TO 314
  300 CONTINUE
  314 KN=N+1
      IB=2
      DO 10 KI=1,N
      I= KN-KI
      XLAM=Z(KI)
      WL(I)= 100000./XLAM
   13 B=XLAM-V(IB)
      IF(B) 111, 12, 12
   12 IB=IB+1
      GO TO 13
  111 IA=IB-1
      IF(B+XLAM-V(IA)) 14, 15, 15
   14 XMIR=WKK(KI)/F(IA)
      GO TO 21
   15 XMIR=WKK(KI)/F(IB)
   21 E(I)=(R(KI)-W(KI))/(XMIR-W(KI))
   10 CONTINUE
      N1K=10.*WL(1)
      N2K=10.*WL(N)
      MM=N2K-N1K+1
      WS=N1K*.1
      W(1)= WS*.18852
      WC=WL(1)
      WD=WL(2)
      RL=E(1)
      RU=E(2)
      SL=(RU-RL)/(WD-WC)
```

```
      MN=2
      WKK(1)=WS
      R(1)=RL+SL*(WS-WC)
      Z(1)= ALOG(R(1))
      DO 20 I=2, MM
      WS=WS+.100006
      WKK(I)=WS
      W(I)=WS*.18852
      IF(WS-WD) 22, 22, 24
   24 MN=MN+1
      WC=WD
      WD=WL(MN)
      RL=RU
      RU=E(MN)
      SL=(RU-RL)/(WD-WC)
      IF(N-MN)328,702,702
  702 IF(WS-WD)22,22,24
   22 R(I)= RL+ SL*(WS-WC)
   20 Z(I)= ALOG(R(I))
      WL(1)= 100000./WKK(1)
      WL(MM)= 100000./WKK(MM)
      NN=MM-1
      W1=W(1)
      WN= W(MM)
      Z1=Z(1)
      ZN= Z(MM)
      IF(WLA) 241, 240, 241
  240 AA1=Z1
      BB1=ZN
      XRL=0.0
      XRH=0.0
      XLW=0.0
      XHW=0.0
      GO TO 242
  241 WKA= 100000./WLA
      WKB= 100000./WLB
      DO 30 L=1, MM
      IF(WKA-WKK(L)) 31, 31, 30
   31 LA=L
      GO TO 32
   30 CONTINUE
   32 DO 33 L=1,MM
      IF(WKB-WKK(L)) 34, 34, 33
   34 LB=L
      GO TO 35
   33 CONTINUE
   35 DO 140 I=1, 2
      IF(I-1) 141, 141, 142
  141 II=LA
      GO TO 143
  142 II=LB
  143 ZI= Z(II)
      WI= W(II)
      WP1= W1+ WI
      WM1= W1-W1
```

```
      WPN= WN+WI
      WMN= WN-WI
      D=((ZI-ZI)/(WP1*WM1)+ (ZI-ZN)/(WPN*WMN))/2.
      DO 211 J=2, NN
      IF(II-J) 271, 941, 271
  941 KM= II-1
      KP= II +1
      SHIP= ((ZI-Z(KM))/((W(KM)+WI)*(W(KM)-WI))+(ZI-Z(KP))
     2 /((W(KP)+WI)*(W(KP)-WI)))/2.
      RI= R(II)
      CH= .019852
      CM= (R(KP) -R(KM))*26.593
      CMR= CM*(4.*CM*WI  -RI)
      SHEP=CM*WI*(CH*CMR +(CMR*WI +3.*RI*RI)*ALOG((2. *WI -CH)/
     2 (2.*WI +CH)))/(9.42477*RI*RI*RI)
      D= D +SHEP/CH -SHIP
      GO TO 211
  271 D= D+ (ZI-Z(J))/ ((W(J) +WI)*(W(J)-WI))
  211 CONTINUE
      D=D*0.18852
      IF(I-1) 161, 161, 162
  161 DKA= THA- WI*D/31.416
      DXA=          ALOG(WP1/WM1)/6.2832
      DZA=          ALOG(WMN/WPN)/6.2832
      ZIA=ZI
      GO TO 140
  162 DKB= THB- D*WI/31.416
      DXB=          ALOG(WP1/WM1)/6.2832
      DZB=          ALOG(WMN/WPN)/6.2832
      ZIB=ZI
  140 CONTINUE
      DAA=DKA +ZIA*( DXA +DZA)
      DBB=DKB +ZIB* (DXB +DZB)
      AA1=(DBB -(DAA*DZB) /DZA) / (DXB -(DXA* DZB) / DZA)
      BB1=(DAA-AA1*DXA)/DZA
      XRL=2.718**AA1
      XRH= 2.718**BB1
      XLW= (AA1 -ZIA) *DXA
      XHW= (BB1 -ZIB) *DXB
  242 CONTINUE
      WRITE(6,61) TITLE,C,N,WLA,THA,WLB,THB,XRL,XLW,XRH,XHW
   61 FORMAT(1H1,20A4//' MOL CON=',F7.4,31X,'# DATA  PTS =',I6/
     4 ' WLA=',F6.0,6X,' THETA=',F7.4,20X,' WLB=',F6.0,6X,' THETA=',
     5 F7.4/'  RL=',F6.4,6X,' LWING=',F7.4,20X,'  RH=',F6.4,6X,
     3 ' HWING=',F7.4,          //5X,' EXTC(10-3)',4X,' LOGWND',
     15X,' CIRCFREQ',4X,' PHASE',9X,' N',9X' K',4X,' WAVEL(A)',4X,
     2' WAVFN(KK)',4X,' REFLECT'//)
      DO 40 I=2,NN
      ZI=Z(I)
      WI=W(I)
      WP1=W1+WI
      WM1=WI-W1
      WPN=WN+WI
      WMN= WN-WI
      D= ((ZI-ZI)/(WP1*WM1) +(ZI-ZN)/(WPN*WMN)) /2
```

```
      DO 11 J=2,NN
      IF (I-J) 71,41,71
   41 KM=I-1
      KP=I+1
      SHIP= ((ZI-Z(KM))/((W(KM)+WI)*(W(KM)-WI))+(ZI-Z(KP))
     2 /((W(KP)+WI)*(W(KP)-WI)))/2.
      RI= R(I)
      CH= .018852
      CM= (R(KP) -R(KM))*26.593
      CMR= CM*(4.*CM*WI  -RI)
      SHEP=CM*WI*(CH*CMR +(CMR*WI +3.*RI*RI)*ALOG((2. *WI -CH)/
     2 (2.*WI +CH)))/(9.42477*RI*RI*RI)
      D= D +SHEP/CH -SHIP
      GO TO 11
   71 D= D +(ZI-Z(J))/((W(J) +WI)*(W(J) -WI))
   11 CONTINUE
      D= D*.18852
       UP=(D*WI*.2+ (AA1-ZI) *ALOG(WP1/WM1)+(BB1-ZI)  *ALOG(WMN/WPN))/
     1  6.2832
      RI=R(I)
      WL(I)= 100000./WKK(I)
      US= -2.0*SQRT(RI)
      UB= US*COS(UP) +RI
      UN= (1.0-RI)/ (1.0+UB)
      UK= US*SIN (UP)/ (1.0+UB)
      UWN= WKK(I)
      ULWN= ALOG10(UWN) + 3.0
      UEX= -545650.*UK/(WL(I)*C)
      E(I)= UEX
      WRITE(6,64) UEX,ULWN,WI,UP,UN,UK,WL(I),UWN,R(I)
   64 FORMAT(1X,F15.6,4X,F7.4,5X,F8.5,4X,F7.4,4X,F7.4,4X,F7.4,5X,F8.0,
     16X,F8.4,4X,F8.6)
      IF (MG) 40, 40, 27
   27 WRITE(7, 62) UWN, WL(I), ULWN, UEX
   62 FORMAT (4F10.5)
   40 CONTINUE
      DO 601 K= 2, 102
  601 LPOT(K)= LDT
      LPOT(1)= LXI
      LPOT(103)= LXI
      ETOP= 0.
      E(1)= 0.
      E(MM)= 0.
      DO 610 K= 2, NN
      IF(ABS(E(K))-ETOP)610,610,612
  612 ETOP=ABS(E(K))
  610 CONTINUE
      RTOP= R(1)
      DO 810 I= 1, MM
      IF(R( I)- RTOP) 810, 810, 812
  812 RTOP= R( I)
  810 CONTINUE
      WRITE(6, 631) RTOP, ETOP, LPOT
  631 FORMAT(1HI, 10X,' (*) REFLECTANCE 100%=',F10.5,20X,
     5 ' (+) EXTINCTION COEF 100%=',
```

```
   2       F10.5// ' WNO(KK)', ' 0°,7X,' 10°, 7X, ' 20°, 7X, ' 30°,
   3 7X, ' 40°, 7X, ' 50°, 7X, ' 60°, 7X,  ' 70°, 7X, ' 80°, 7X,
   4 ' 90°, 6X, ' 100°, ' WL(A)'/8 X, 103A1)
    DO 644 K=2, 102
644 LPOT(K)= LBB
    DO 700 K= 1, MM
    JR= R(K)*100.0/ RTOP +2.5
    JE= E(K)*100./ETOP
    IF(JE) 621, 622, 622
621 JE= 2.5 -JE
    LPOT(JE)= LXB
    GO TO 623
622 JE= JE+ 2.5
    IF(JR-JE) 625, 626, 625
626 LPOT(JR)= LXX
    GO TO 627
625 LPOT(JE)= LPL
623 LPOT(JR)= LST
627 WRITE(6, 630) WKK(K), LPOT, WL(K)
630 FORMAT(1X, F7.1, 103A1, F6.0)
    LPOT(JE)= LBB
700 LPOT(JR)= LBB
    GO TO 4
328 STOP
    END
```

APPENDIX C

PREPARATION OF OTHER BDP^+ SALTS

BDP^+Br^- was prepared by the same procedure as BDP^+Cl^- except that the ion exchange column was washed with a NaBr solution rather than a NaCl solution (see chapter II). When BDP^+Br^- is recrystallized from 95% ethanol, a bright yellow solid is obtained which melts from 92 to 95°C: recrystallization from absolute ethanol and anhydrous ether produces an orange colored solid which melts from 200 to 202.5°C. These forms are interconvertible simply by changing back and forth from 95% ethanol to absolute ethanol. If a small amount of water is added to the orange solid, it turns yellow immediately. A yellow form of the compound is also obtained when methanol is used as the solvent.

BDP^+I^- was prepared from BDP^+Cl^- making use of the fact that potassium iodide is soluble in alcohol but insoluble in ether. Accordingly, a small amount of BDP^+Cl^- was dissolved in ethanol, and a solution of KI in ethanol was added until precipitation was complete. The precipitate (KCl) was removed, and diethyl ether was added to the super-

natant solution. A bright yellow flocculent precipitate (BDP^+I^-) formed. The compound was recrystallized by dissolving it in ethanol and adding ether. The purified material melts at 224 to 226°C. The crystal density of BDP^+I^- is 1.503 gram per milliliter. X-ray analysis performed with the assistance of Dr. Dick van der Helm indicated the crystal space group is $P2_1/c$ with cell dimensions a=6.345, b=13.905, and c=13.951 Å, α=89.9°, β=83.8°, and γ=89.89°. The volume of the unit cell is 1223.6 $Å^3$. The cell volume and density implies four molecules per unit cell. Crystals of the Br^- and I^- salts were grown by the same procedure used for the Cl^- salt.

The sulfate salt was prepared by the same procedure used for the Cl^- and Br^- salts; however, it is more difficult to crystallize. An oil is obtained in which crystals will form, but they are generally low quality crystals.

BIBLIOGRAPHY

1. R. W. Ditchburn, Light, 2nd. Ed., Interscience Publishers, New York, 1963, pp. 535, 553, and 591.
2. W. R. Hunter, J. Opt. Soc. Am. 55(10), 1197 (1965).
3. S. P. F. Humphreys-Owen, Proc. Phys. Soc. (London)77, (1961).
4. G. Andermann, A. Caron, and D. A. Dows, J. Opt. Soc. Am. 55(10), 1210 (1965).
5. Che-Kuang Wu and G. Andermann, J. Opt. Soc. Am. 58(4), 519 (1968).
6. L. P. Mosteller Jr. and F. Wooten, J. Opt. Soc. Am. 58(4), 511, (1968).
7. D. M. Roessler, Brit. J. Appl. Phys. 16, 1119 (1965).
8. D. M. Roessler, Brit. J. Appl. Phys. 16, 1359 (1965).
9. D. M. Roessler, Brit. J. Appl. Phys. 17, 1313 (1966).
10. G. Feniak, Ph.D. Dissertation, University of Washington, 1955.
11. S. C. Neely, Ph.D. Dissertation, Yale University, 1965.
12. S. S. Malhotra and M. C. Whiting, J. O. A. C. (1960).
13. B. G. Anex and W. T. Simpson, Rev. Mod. Phys. 32, 466 (1960).

14. M. Gottlieb, J. Opt. Soc. Am. 50, 343 (1960).

15. L. B. Clark and M. R. Philpott, J. Chem. Phys. 53, 3790 (1970).

16. J. Homer, Unpublished research.

17. M. Born and E. Wolf, Principles of Optics, 4th Ed., Premagon Press (1970), pp. 627 and 40.

18. M. Pelczar Jr. and R. Reid, Microbiology, 2nd Ed., McGraw Hill, 1965.

19. A. V. Fratini, Ph.D. Dissertation, Yale University, 1966.

20. Handbook of Chemistry and Physics, 48th Ed., The Chemical Rubber Co., 1968, page A-248.

21. J. Vincent-Geisse, Nguyen Tan Tai, and J. P. Pinan-Lucarre, Le Journal De Physique 28, 26 (1967).

22. T. S. Robinson and W. C. Price, Molecular Spectroscopy edited by G. Sell (The Institute of Petroleum, London) 1955.

23. P. N. Schatz, S. Maeda, and K. Kozima, J. Chem. Phys. 38, 2658 (1963).

24. J. S. Plaskett and P. N. Schatz, J. Chem. Phys. 38 612 (1963).

25. J. C. Phillips, Solid State Physics 18, F. Seitz and D. Turnbull, Eds., Academic Press Inc., New York (1966).

26. B. M. Fanconi, G. A. Gerhold, and W. T. Simpson, Molecular Crystals and Liquid Crystals 6, 41 (1969).

27. M. R. Philpott, J. Chem. Phys. 54, 2120 (1971).

28. J. Vincent-Geisse and J. Lecomte, Applied Optics 1, 575 (1962).

29. D. W. Barnes and P. N. Schatz, J. Chem. Phys. 38, 2662 (1963).